

Planning, Dimensioning, and Economic Assessment of Bidirectional Thermal Networks with Prosumers

Master's Thesis

In partial fulfillment of the requirements for the degree
Master of Science
At the School of Engineering and Design of the Technical University of Munich.

Advisor M.Sc. Thomas Licklederer
Prof. Dr. Thomas Hamacher
Munich Institute of Integrated Materials, Energy and Process Engineering

Submitted by
Fabian Johannes Speer




Submitted on Munich, 19.03.2023

Abstract

The energy and mass flows in prosumer-based thermal networks (PBNs) are bidirectional and volatile; thus, dimensioning methods for conventional unidirectional thermal networks (CNs) are not directly applicable. Statements on PBN component sizes and network costs are usually based on elaborate thermohydraulic simulations. However, a way to quickly compare the economic performance of PBNs and CNs for variant decisions in early project phases is desired. After qualitatively comparing the performance and dimensioning approaches of the two network variants, this thesis proposes a rule-based method to determine the relevant maximal power flows through each pipe section of the network. Based on this, the design parameters for network pipes, control valves, and circulation pumps are dimensioned for a line PBN in which each prosumer is connected with a single branch pipe directly to the main distribution pipeline. The required inputs for the method are the secondary side prosumer characteristics and the targeted network conditions, like pressure gradient and temperature levels. The method is implemented in an Excel tool with macros, and its application is demonstrated on a case study network with five residential prosumers. The method's accuracy and the functionality of the dimensioned components are analyzed with a Modelica-based thermohydraulic grid model simulated in the Dassault Systèmes software Dymola. The validation criteria were (i) the accuracy of the predicted design power flows, (ii) a sufficient supply of consumers regarding the transferred power and secondary supply temperature, and (iii) the correct behavior of valve opening, pump speed, and comparison of actuator operating state during design load conditions. Criteria (i) and (ii) were fulfilled with minor deviations. The analysis of criterion (iii) revealed that the design network states could not be fully achieved due to the chosen control strategy. However, all actuators remained in operable ranges, and the recorded divergences did not impair the network's functionality. Thus, the introduced method produced functional component sizes for the case study PBN. A CN variant was designed with established dimensioning methods in the same boundary conditions for an economic comparison and sensitivity analysis of the two network types. In the PBN variant, the annual capital-related costs were 17 %, and the operation-related costs were 25 % higher than in the CN variant. In the base scenario, the PBN needs to reduce demand-related costs by 21 % compared to the CN to be economically viable. Rising network lengths, energy prices, and full-load hours would benefit the viability of the PBN. However, a growing interest rate would increase the viability of the CN. Aspirations for climate neutrality, energy price developments, and advances in control strategies are expected to benefit the future relevancy of PBNs.

Statement of Academic Integrity

I,

Last name: Speer
First name: Fabian Johannes
ID No.: 

Hereby confirm that the attached thesis,

Planning, Dimensioning, and Economic Assessment of Bidirectional Thermal Networks with Prosumers

Was written independently by me without use of any sources or aids beyond those cited, and all passages and ideas taken from other sources are indicated in the text and given the corresponding citation.

I confirm to respect the „Code of Conduct for Safeguarding Good Academic Practice and Procedures in Cases of Academic Misconduct at Technische Universität München, 2015“, as can be read on the website of the Equal Opportunity Office of TUM.

Tools provided by the chair and its staff, such as models or programmes, are also listed. These tools are property of the institute or of the individual staff members. I will not use them for any work beyond the attached thesis or make them available to third parties.

I agree to the further use of my work and its results (including programmes produced and methods used for research and instructional purposes.

I have not previously submitted this thesis for academic credit in any study program.

In agreement with the supervisor, parts of this thesis were published as a conference paper for the IEWT2023 conference in Vienna. It is available at:

https://iewt2023.eeg.tuwien.ac.at/download/contribution/fullpaper/104/104_fullpaper_20230210_224423.pdf

Munich, March 19, 2023.

(Author: Speer, Fabian Johannes)

Contents

Abstract.....	I
Statement of Academic Integrity	III
List of Figures	VI
List of Tables	VII
List of Abbreviations and Symbols	VIII
1. Introduction	1
2. State of the art	2
2.1. Conventional thermal networks	2
2.2. Prosumer networks	4
2.2.1. Prosumers in thermal networks.....	4
2.2.2. Challenges of prosumer integration	4
2.2.3. Design approaches	6
3. Research questions and methodology	8
3.1. Research questions	8
3.2. Methodology	9
3.3. Scope of investigations	9
3.4. Structure of this thesis	10
4. Qualitative comparison.....	11
4.1. Strengths and weaknesses	11
4.1.1. Prosumer networks	11
4.1.2. Conventional networks.....	12
4.1.3. Comparison	12
4.2. Economic sensitivities	14
5. Adaptation of planning methods	15
5.1. Dimensioning approach	16
5.2. Dimensioning tool for line prosumer-based networks	17
5.2.1. Conditions and assumptions	17
5.2.2. Component Dimensioning.....	18
6. Dimensioning the case study networks	22
6.1. Network characteristics	22
6.2. Prosumer characteristics.....	23
6.3. Component dimensioning	23
6.3.1. Prosumer-based network.....	24
6.3.2. Conventional network	25
6.3.3. Comparison	27
7. Tool validation - Dymola simulation.....	29
7.1. Exchange scenarios.....	30
7.2. Results.....	33

8. Economic analysis	38
8.1. Investment costs and annuity	38
8.2. Sensitivity analysis	41
8.2.1. Sensitivity of capital- and operation-related costs.....	41
8.2.2. Sensitivity of demand-related costs.....	42
9. Conclusion and outlook	45
9.1. Conclusion	45
9.2. Outlook	47
References.....	X
Appendix.....	XV
A. Economic analysis.....	XV
B. Dimensioning tool	XIX
C. Simulation parameters.....	XXV

List of Figures

Figure 1: Comparison of pressure curves and hydraulic circuits in different operation states of CNs and PBNs central generation unit (A and B) vs. prosumer-based network (C and D) (own figure).....	5
Figure 2: Methodology of the thesis	9
Figure 3: Structure and nomenclature of a line prosumer-based network.....	15
Figure 4: Algorithm for determining the design power flow for network pipes in line PBNs	16
Figure 5: Flow chart for component design in the dimensioning tool	19
Figure 6: Recommended components for a CN substation [84]	25
Figure 7: Sizes of the dimensioned piping sections in the PBN and CN	27
Figure 8: Dimensioned pump heads for the PBN FIPs and the central CN pump.....	28
Figure 9: Section of the case study PBN model in Dymola.....	29
Figure 10: Qualitative pressure curves and DHCs for pumps and control valves in the exchange scenarios 1 to 4	31
Figure 11: Prosumer load situations during the exchange scenarios.....	32
Figure 12: Absolute errors for simulated power and volume flow compared to design power and volume flow in the PBN network pipes	33
Figure 13: Errors for simulated and designed values for consumption power and secondary supply temperature during design and part load consumption scenarios	34
Figure 14: Absolute error for the primary side temperature spread across all scenarios.	35
Figure 15: Pump curves at maximal pump speed and dimensioned and simulated operating points of FIPs and CoVs during design states.....	36
Figure 16: Comparison of the investment costs of the PBN and CN case study networks	38
Figure 17: Comparison of the annual capital-related costs of the PBN and CN case study networks	39
Figure 18: Comparison of the annual operation-related costs of the PBN and CN case study networks	40
Figure 19: Sensitivity analysis for the annual costs of the PBN (solid lines) and CN (dashed lines) for changing interest rate and network section length	41
Figure 20: Comparison of the annual capital- and operation-related costs of the PBN and CN - including heat generators.....	43
Figure 21: Needed reduction in demand-related costs in the PBN to break even with the annual CN costs - sensitivity analysis for full-load hours and energy cost.....	44

List of Tables

Table 1: Relative comparison of strengths and weaknesses of CNs and PNs; CN:“0” and PN:“+“ or “-“ for minor differences; CN:“+“ or “-“ and PN: “+“ or “-“ for greater differences	13
Table 2: Influencing factors on economic efficiency and the sensitivity of CNs and PNs “--” Very sensitive, “-“ sensitive, “0” not very sensitive	14
Table 3: Network parameters used for dimensioning the case study	22
Table 4: Length of network routes in the conventional and prosumer-based network	23
Table 5: Prosumer characteristics applied in the case study	23
Table 6: Heat exchanger dimensions in the PBN and the CN.....	24
Table 7: Manufacturers and product lines used in the PBN case study	24
Table 8: Pipe dimensions and designed power and volume flows in the PBN	24
Table 9: Control valve dimensions and designed operating points in the PBN.....	25
Table 10: Pump dimensions and designed operating points in the PBN	25
Table 11: Manufacturers and product lines used in the CN case study.....	26
Table 12: Pipe dimensions and designed power and volume flows in the CN.....	26
Table 13: Belimo energy valve dimensions and designed operating points in the CN.....	26
Table 14: Pump dimensions and designed operating points in the CN	26
Table 15: Applied weighting for the target values of the four PID controllers [54] in all prosumers	30
Table 16: Design scenarios for the actuators.....	32
Table 17: Normalized speed of FIPs and opening of CoVs at their operating points.....	35
Table 18: Chosen Vaillant [90] heat generators for the economic analysis of the case study PBN and CN.....	42
Table A.1: Investment costs of the case study PBN	XV
Table A.2: Investment costs of the case study CN	XVI
Table A.3: Used life cycles and yearly operational costs, based on the VDI2067	XVII
Table A.4: Data points considered in the economic analysis; AI: analog input, AO: analog output, DI: digital input, DO: digital output	XVIII
Table B.1: Pseudo-code nomenclature.....	XIX
Table C.1: Set power transfers (exchange scenarios) at the prosumer substations in the simulation negative value: consumption-mode, positive value: Production-mode	XXV
Table C.2: Applied parameters for the ProsNet [51] models and PID controllers [54] in the Dymola simulation.....	XXVI

List of Abbreviations and Symbols

Abbreviations	Meaning
ANE	All-Neighbor-Exchange
CN	Conventional thermal network
ConP	Consumption pump
CoSES	Combined Smart Energy Systems
CoV	Control valve
DHC	Design hydraulic circuit
DHW	Domestic hot water
DN	Nominal size
FIP	Feed-in pump
GA	Genetic algorithm
GHG	Greenhouse gas
HWP	Hydraulic worst point
MAS	Multi-agent systems
MILP	Mixed-integer linear programming
ML	Machine-learning
MPC	Model predictive control
ONE	One-Neighbour-Exchange
PBN	Prosumer-based thermal network
PJP	Plastic jacket pipe
PN	Thermal network with prosumers
ProP	Production pump
Pros	Prosumer
RN	Reservoir network
Sc	Exchange scenario
SH	Space heating
VBA	Visual Basic for Applications

Symbols	Meaning	Unit
l	Length	[m]
R	Pressure gradient	[Pa/m]
Δp	Differential pressure / pressure loss	[kPa]
H	Pump head	[kPa]
ϑ	Temperature	[°C]
T	Temperature	[K]
a	Valve authority	[-]
P	Thermal prosumer power	[W]
\dot{Q}	Heat flow rate	[W]
\dot{V}	Volume flow rate	[m ³ /h]
\dot{m}	Mass flow rate	[kg/s]
d	Diameter	[mm]
u	Flow velocity	[m/s]
u^{FIP}	Normalized pump speed	[-]
κ^{CoV}	Normalized valve opening	[-]
K_{vs}	Flow coefficient at maximum valve opening	[m ³ /h]
K_v	Flow coefficient of a valve	[m ³ /h]
λ	Friction factor	[-]
I	Investment costs	[€]
r	Interest rate	[%]
L	Life cycle	[a]
A	Annuity	[€/a]
ε	Absolute pipe roughness	[mm]
ρ	Density	[kg/m ³]
c_p	Specific heat capacity	[kJ/(kg K)]
ν	Kinematic viscosity	[m ² /s]

Sub- and superscripts	Meaning
<i>cct</i>	Connection
<i>dis</i>	Distribution
<i>con</i>	Consumption
<i>pro</i>	Production
<i>tar</i>	Target
<i>prim</i>	Primary side
<i>sec</i>	Secondary side
<i>pros</i>	Prosumer
<i>HE</i>	Heat exchanger
<i>ir</i>	Individual resistor
<i>r</i>	Right
<i>l</i>	Left
<i>i</i>	Pipe section number
<i>j</i>	Prosumer number
<i>real</i>	Actual
<i>route</i>	Network route
<i>pipe</i>	Network pipe
<i>des</i>	Design
<i>CenP</i>	Central Pump
<i>theo</i>	Theoretical
<i>set</i>	Set point
<i>SN</i>	Subnetwork
<i>sim</i>	Simulation
<i>FIP</i>	Feed-in-pump
<i>maint</i>	Maintenance
<i>insp</i>	Inspection
<i>s</i>	Servicing

1. Introduction

The European Green Deal specified the carbon neutrality goals in the EU for 2030 and 2050. Until 2030 carbon emissions shall be reduced by at least 50 % compared to 1990, and climate neutrality is to be achieved until 2050. [1] Buildings account for 40 % of end energy usage and 36 % of energy-related greenhouse gas (GHG) emissions [2]. Of that, 79 % is due to space heating (SH) and domestic hot water (DHW) alone [3]. The transition towards renewables in the heating sector is progressing slowly. Renewables provided only 23 % of consumption in the heating and cooling sector in 2020 [4]. District heating networks have the potential to reduce fuel demands and CO₂ emissions significantly [5]. Yet, only about 12 % of the heat volume in Europe is supplied by district heating [6].

With a rising level of urbanization in Europe, the share of the population living in urban areas is expected to grow from 74 % to 84 % by 2050 [7], and the potential for implementing district heating solutions in high-density areas can be expected to increase accordingly. Many decentral energy sources on different temperature levels are available in urban areas. These include excess heat from the industry sector or cooling applications at a lower temperature level, e.g., from data centers and supermarkets [8]. Furthermore, ambient heat sources, such as rivers, lakes, or underground structures, can be exploited with heat pumps and integrated into district heating grids. Investigations for London and Hyllie (a city district in Malmö) even estimated the excess heat potential to be larger than the total demand [9, 10]. Integrating decentral energy sources leads to multiple feed-in points and prosumer participation in district heating networks. To prioritize the different energy sources and to match the demand and supply holistically, the district heating sector needs to become smart. With the increasing electrification of the heat sector and the rising share of fluctuating renewables in electricity generation, demand for grid-supportive sector coupling grows. [11, 12]

Smart thermal grids with prosumers allow a cascading usage of the most energy-efficient and economical heat sources to meet variable demand. This would automatically prioritize renewable energy sources and minimize CO₂ emissions. [13, 14]

Furthermore, diurnal thermal storage in smart networks enables peak load shifting and reduces stress on the electricity and thermal grid [15]. However, due to the various modes of operation, increased volatility, and the different technical infrastructure requirements in thermal networks with prosumers (PN), previous dimensioning methods for conventional networks (CN) cannot be applied directly but must be adapted.

2. State of the art

Since the 1800s, district heating networks have evolved through multiple generations. Improvements in heat source-, storage-, and distribution technologies, as well as lower temperatures in the grid, resulted in increased efficiencies and reduced losses. Lund et al. divided these developments into four generations [16]. The first three generations strictly featured centralized generation and central pumps to distribute the heat carrier, while decentral pumps and heat sources started to be integrated into grids of the 4th generation. In recent years the term “5th generation district and cooling networks” has been established in publications [17–20]. In the context of these investigations, increasing emphasis was put on the integration of distributed thermal sources and prosumers, the operation at ambient temperature levels, and the combined supply of heat and cold in one network. However, there are no clear definitions for the characteristics of 5th generation networks, and the term itself still faces controversial opinions [19, 20]. Lindhe et al. argued that the main differentiating factors should be the possibility to provide heating and cooling simultaneously and the disconnect between network temperature and secondary side supply temperature caused by heat pumps [20].

2.1. Conventional thermal networks

In CNs, a central generation unit provides thermal energy for all connected consumers. A central circulation pump station drives a unidirectional mass flow in a network of supply and return pipes to distribute the energy carrier to the consumers. Depending on the operating temperatures and the type of piping, CNs can be categorized into the 1st to 4th district heating generation [16].

Dimensioning methods for the components in CNs are well-documented and established. Multiple planning guidelines from manufacturers [21, 22] and institutions [23–25], various standards [26, 27], and comprehensive statistical data [24, 28] are available. The usual main steps for the hydraulic dimensioning of core network components, i.e., pipelines, control valves, and circulation pump(s), can be summarized as follows:

1. Pipe dimensioning:

Due to the unidirectional mass flow and central generation in conventional networks, the relevant design state for the pipes is defined by the maximum consumption power of the downstream consumers. With the temperature difference for supply and return pipes, the relevant volume flow is calculated, and subsequently, the pipe diameter can be designed for a defined maximum pressure gradient. [23]

2. Control valve (CoV) dimensioning:

The pressure gradient in pipelines and miscellaneous fittings determines the pressure losses in the hydraulic circuits from the central plant to the consumers. The CoV at the consumers is then dimensioned for an aspired valve authority. [23]

3. Pump dimensioning:

Considering simultaneity factors, the total consumer demand describes the volume flow the central pumping station must provide. The pump head is dimensioned for the differential pressure needed in the hydraulic with the highest pressure losses. This is usually the circuit to the consumer farthest from the central plant. The grid's total pressure levels are then specified considering the network's geodetic conditions. [23]

Buffa et al. described multiple control strategies, which usually operate simultaneously in CNs. At a pump station level, the control strategies are (i) the supply temperature control to ensure satisfying temperatures for all consumers, (ii) the minimum differential pressure control to ensure sufficient flow at the consumers, and (iii) the minimum and maximum pressure control to protect the pump from cavitation and other components from damage by overpressure. [29]

At a substation level, the heat demand and flow control ensure the sufficient supply of the secondary side consumer by modulating the primary side volume flows. [29]

Current research on CNs is oriented toward optimizing component sizing [13, 30–34] and control strategies to reduce overall costs and losses [35–37].

2.2. Prosumer networks

2.2.1. Prosumers in thermal networks

There are multiple types of networks with thermal prosumers and diverse ways to connect prosumers hydraulically. The main distinguishing points are (i) the number of pipelines at different temperature levels, (ii) the directionality of mass flow due to central or decentral pumps, (iii) the way prosumers are connected to the network pipelines, (iv) the possibility for cooling, and (v) the role of centralized entities. Generally, these network types would be categorized as either 4th generation or 5th generation networks depending on temperature levels and possibilities for energy exchange or combined heat and cold production [16, 20].

An example of a single-pipe prosumer network is the reservoir network (RN) with centralized pumps described by Sommer et al. [38]. For a two-pipe network with unidirectional central pumps, Ancona et al. compared four different connection types of a prosumer [39] and chose a return-to-supply configuration as the best option for their experimental substation [40]. Lickleder et al. described a two-pipe system featuring bidirectional mass flow in the cold and hot subnetworks with decentral pumps and a complete lack of central entities, where prosumers are connected indirectly with a heat exchanger [41]. Stanica et al. developed a cascading three-pipe prosumer network with three temperature levels featuring partially bidirectional and partially unidirectional mass flows [42]. For the SCENIC project, Jones et al. proposed a novel four-pipe prosumer network with two loops. A network loop to supply heat and a generation loop to collect energy from distributed heating systems [43]. Both operate with a unidirectional flow driven by central pumps [43].

2.2.2. Challenges of prosumer integration

Integrating prosumers into thermal networks proved to be a non-trivial task. Multiple sources have reported challenges regarding hydraulic behavior and control strategies caused by distributed generation and the associated flow reversals.

Brange et al. described different scenarios in which distributed generation could lead to too low differential pressures for consumers when using a differential pressure control for the circulation pumps [44, 45]. The investigations of Hassine et al. on the integration of distributed solar heat suppliers had similar findings [46]. It was concluded that conventional, differential pressure-driven control strategies do not guarantee safe operation [46]. In this case, the main problem is that the consumer's position with the lowest differential pressure, the so-called hydraulic worst point (HWP), changes depending on the active prosumer and the amount of supplied heat [15, 42, 46].

The qualitative depiction of pressure curves in CNs and prosumer-based networks in different operation states shows examples of changing HWP (see Figure 1).

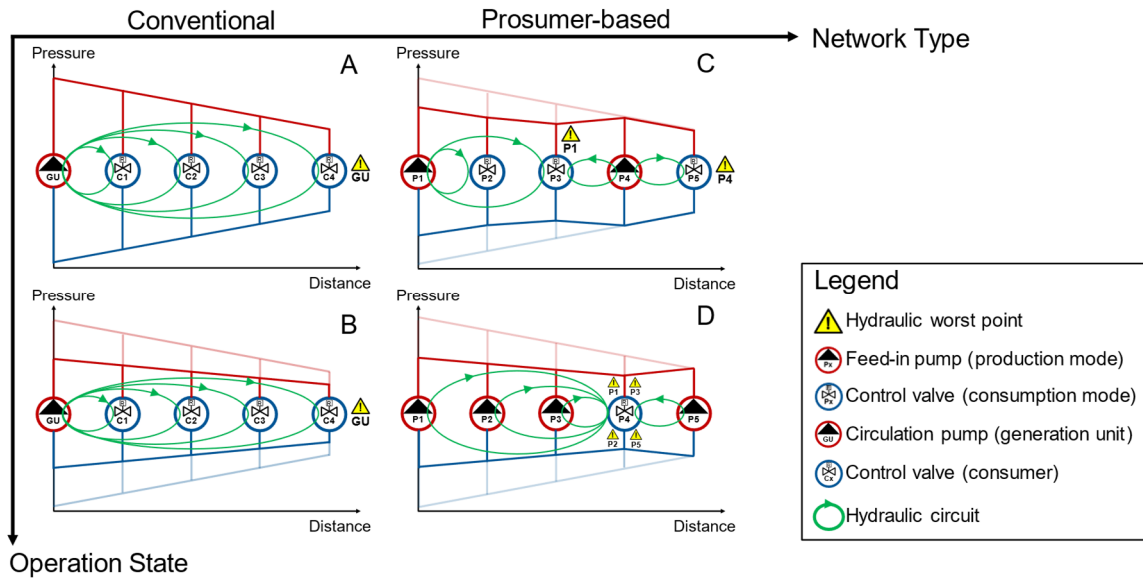


Figure 1: Comparison of pressure curves and hydraulic circuits in different operation states of CNs and PBNs central generation unit (A and B) vs. prosumer-based network (C and D) (own figure).

Changing demand in CNs does not cause the hydraulic circuits or HWP to change (see Figure 1, A and B). Changing operation states in prosumer-based networks can cause multiple sub-networks to form, splitting the whole network into smaller hydraulic circuits (see Figure 1, C and D) with internal production and consumption [47].

Additionally, all decentral actuators (pumps and control valves) mutually influence each other due to their influence on the overall network state [47]. This characteristic results in multiple peculiarities of prosumer networks. For example, if multiple feed-in pumps operate simultaneously, one pump can block out another, greatly influencing its mass flow rate or even causing reverse flow in the blocked pump [38, 47, 48]. When two pumps compete to supply a consumer, supply frontiers can develop, halting the mass flow and causing the network temperatures to cool down locally [47].

If only one control valve starts to close due to changing demand, it affects the pressure in the warm network side almost immediately. All substations must react to this by adjusting pump speed or valve position. Since the control loops for mass flow and pressure are tightly coupled, the near-instantaneous pressure change causes challenging control conditions. Such rapid pressure changes can result in high water flow variations and pressure surges in the system, which can cause damage to network components. [48, 49]

These phenomena were observed in model calculations [47, 48, 50] and a real-world example [38] of bidirectional networks.

2.2.3. Design approaches

To overcome the challenges of prosumer integration described above, multiple models were built to depict the complex thermohydraulic behavior of thermal networks with prosumers. Lickleder et al. proposed the mathematical model ProHeatNet_Sim of prosumer-dominated thermal networks with non-directional flows and implemented it in Python [41]. This model was used to validate the Modelica library ProsNet, which enabled dynamic simulations in Dymola [51]. Kauko et al. [8, 15] and Schweiger et al. [52] also built Modelica models and used Dymola for dynamic simulations of thermal networks with prosumers. Other capable modeling and simulation environments used for thermal networks include, for example, Matlab, Simulink, IDA-ICE, TRNSYS, and Simscape [20, 52, 53]. Comparisons and investigations of modeling and simulation environments for district heating networks, however, concluded the Modelica language to be advantageous for multi-domain modeling, modularity, and flexibility [20, 52].

To create smart energy systems, advanced control strategies must be integrated into the PNs on top of existing control strategies in CNs [29]. Lickleder et al. proposed a control approach with four weighted PID controllers per prosumer substation (two controlling consumption- and two controlling production-mode). For each controller, a temperature and a power target are set. The temperature and power errors can be weighted to prioritize reaching one of the two set points. [54]

Buffa et al. described multiple advanced control approaches in their bibliographic study [29]. Strategies with Model predictive control (MPC), mixed-integer linear programming (MILP), machine learning (ML) models, and multi-agent systems (MAS) control are often used for investigations on prosumer network control [29]. Optimizing energy system sizes is often done by applying MILP and genetic algorithm (GA) on district heating grids. Zeng et al. used GA to optimize the pipe diameter of district heating and cooling piping networks [55], while Wang et al. applied GA to optimize the hydraulic design of distributed variable speed pumps in multi-source district heating systems [35]. Multiple other elaborate optimization models have been built to optimize stability [56], energy demand [14], and life cycle costs [57] or to reduce peak loads [58] and CO₂ emissions [57] of thermal prosumer networks [40]. Common problems for modern control and optimization models are the missing standardization for development and communication, as well as the time-consuming and complicated application [29, 52].

Experiences with the operation and planning of real-world thermal prosumer networks are minimal, and no dimensioning guidelines exist [17]. The majority of available information on the planning and design of thermal networks with prosumers derives from the presented theoretical modeling and simulation work, general reviews of the limited existing networks [17, 18, 59], or conceptual considerations [60]. These concepts usually include a kind of central entity in the network structure for load balancing. Thus, the design conditions described in the available literature are not fully comparable to the prosumer-based network type, which functions without any central entity [41].

3. Research questions and methodology

3.1. Research questions

The literature review in section 2 illustrated the technical differences between CNs and PNs. However, it remains unclear which network type is preferred in which conditions. Thus, the first research question investigates the impact of the peculiarities of the two network types on their performance in various aspects:

1. What are possible **qualitative statements** on the **strengths, weaknesses, and economic performance and sensitivities** of conventional and thermal networks with prosumers?

The different dynamic approaches and the limited experience in planning thermal prosumer networks described in 2.2.3 cause high levels of uncertainty in the dimensioning of such networks [17]. This lack of planning guidelines renders comparisons with other network variants in early design stages challenging and causes decision makers to prefer proven technologies [17]. Thus, the second research question for this thesis originated:

2. Can **conventional dimensioning methods be adapted** for a functional static design of prosumer-based network components with limited information in early project stages?

Building on the second research question, once the component dimensions are established, the economic performance of a network becomes crucial for the judgment of decision makers in variant comparisons. This leads to the third research question:

3. How do prosumer-based networks fare in a comparative **economic analysis** against conventional networks, and how **sensitive** are they to changes in boundary conditions?

The approach to answering these questions is described in the following subsections.

3.2. Methodology

The methodology of this thesis is summarized in Figure 2.

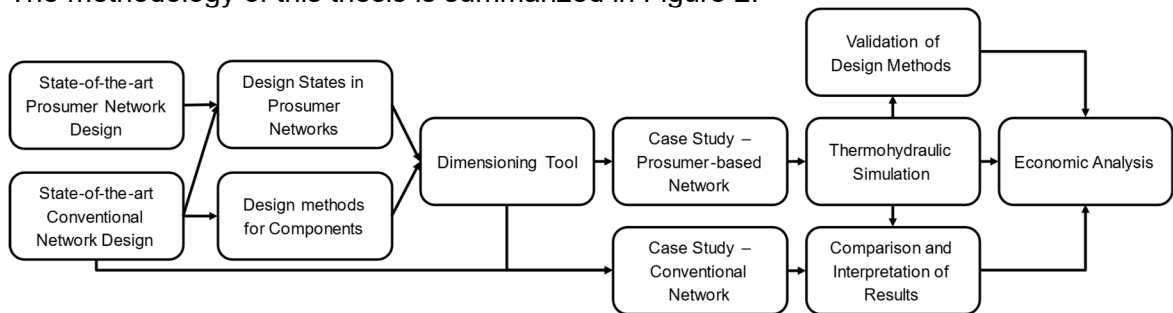


Figure 2: Methodology of the thesis

In more detail, the following steps were performed:

1. Research of state-of-the-art methods on technical planning, dimensioning, and economic efficiency of conventional local thermal networks and thermal networks with prosumers.
2. Elaboration on the essential differences between CNs and PNs regarding technical planning, design, and economic aspects.
3. Development of planning and design methods for bidirectional thermal prosumer networks by adapting existing state-of-the-art methods.
4. Integration of the adapted methods into a dimensioning tool to automate the sizing process for a particular PN structure: prosumer-based networks with bidirectional flow (PBN) described in [41] in a line network typology.
5. Case study: planning and technical design of a CN and a PBN for a fictional line network structure based on the residential prosumers emulated in the Combined Smart Energy Systems (CoSES) center [61].
6. Validation of the adapted methods and dimensioning tool: preparation and execution of a simplified simulation to investigate the network's functionality during different energy exchange scenarios.
7. Economic and sensitivity analysis of the CN and the PBN network variants.

3.3. Scope of investigations

The qualitative investigations on the performance of CNs and PNs in steps 1 and 2 (see subsection 3.2) include all network subtypes because general statements on the consequences of the fundamental structural and operational differences are desired.

Steps 3 to 7 of the methodology focus on a line PBN structure. The line structure is a subtype of a radial network typology in which the prosumers are connected directly to a

main distribution pipeline with single branch pipes. This line PBN structure is described in detail in Chapter 5. The prosumer or consumer conditions are based on the five residential houses emulated in the CoSES lab [61]. Since the focal point of this thesis lies on network infrastructure, the secondary side characteristics are considered only roughly and only if necessary for statements on the network, as further described in Chapters 6 and 8.

In the economic analysis (step 7 in subsection 3.2), the investment costs are derived from real-world offers or manufacturer price sheets, if available. Otherwise, prices are calculated from statistical values or cost catalogs. The annuity costs for capital and operational expenses of the two variants are compared based on the statistical values for life cycles and the percentual operational costs described in the VDI2067. Statements on demand-related costs are derived based on a simplified heat demand calculation (see Chapter 8). The sensitivity analysis of the economic performance is conducted for four influencing factors that do not necessitate adjusted component sizes (see subsection 8.2).

3.4. Structure of this thesis

To answer the three research questions, the thesis is structured as follows:

Chapter 4 focusses on answering the first research question and elaborating on qualitative differences between strengths, weaknesses, and economic sensitivities of PNs and CNs as a conclusion from the literature review in Chapter 2. The findings from Chapters 2 and 4 build the basis for answering the second research question in Chapters 5 to 7. The adapted dimensioning methods and the integration into a dimensioning tool for line PBNs are presented in Chapter 5. Chapter 6 describes how the case study district heating network for five example residential houses is dimensioned for a PBN and a CN structure. The functionality of the dimensioned PBN, and thus, the proposed dimensioning method, is validated with a thermohydraulic simulation of the case study network in Chapter 7. Then, a comparative economic analysis between the PBN with validated component sizes and the CN is described in Chapter 8 to answer the third research question. Ultimately a conclusion is drawn, and an outlook on further research on PBNs is given in Chapter 9.

In agreement with the supervisor, parts of this thesis were published as a conference paper for the IEWT2023 conference in Vienna [62]. It is available at:

https://iewt2023.eeg.tuwien.ac.at/download/contribution/fullpaper/104/104_fullpaper_20230210_224423.pdf

4. Qualitative comparison

The qualitative comparison between CNs and PNs is not limited to one of the network structures described in subsection 2.2.1. Instead, a broad overview of the characteristics, strengths, and weaknesses of PNs, resulting from their fundamental structural and operational differences from CNs, is given.

4.1. Strengths and weaknesses

4.1.1. Prosumer networks

The strengths of PNs are generally tied to their greater modularity and operation flexibility for future development [18]. The increased operation flexibility increases the potential for controlling the pumps and heat generators to operate at their optimal efficiency, especially during extended part-load situations in summer months [63]. Some PNs can provide both heating and cooling to prosumers with only one grid which facilitates the utilization of waste energy and saves infrastructure investment costs [18]. Additionally, a change in building demand can be addressed by decentral changes at the prosumer level, making the whole system more resilient to varying conditions [18]. In PNs, prosumers use a portion of the generated energy locally. Consequently, the amount of heat transported in the grid is reduced. Thus, less energy is lost to the ground, and less energy is required for pumping [64, 65]. Additionally, the resulting reduced mass flows potentially allow the pipe diameters to be dimensioned smaller to further reduce ground losses and decrease investment costs [64]. However, the flexibility of bidirectional energy and mass flows in PNs is also responsible for their weaknesses. For PNs with at least two heat exchangers between the heat source and sink, higher exergy losses than in CNs are inherent [66]. The main challenges of prosumer integration are described in detail in subsection 2.2.2. Apart from these hydraulic and control-related challenges, different economic weaknesses can be attributed to PNs. Generally, higher investment costs for advanced substations, complex planning, and multiple feed-in pumps are needed [17, 18, 67]. Furthermore, a more frequent change of power levels or operation mode can increase maintenance costs or decrease the life cycles of components [63]. On top of that, the billing and ownership structures in PNs are more complex and not yet commonly established [17].

4.1.2. Conventional networks

The strengths of CNs result from their centralized generation and simple operating principle. Firstly, with centralized components, there is a reduced maintenance effort due to fewer actuators with moving parts and, thus, fewer points of failure [49, 68]. The limited amount of actuators, the unidirectional mass flow, and simplified substations simultaneously reduce investment costs and facilitate control strategies [29]. Generally, the larger generation units in CNs are more cost-efficient regarding the investment costs per *kW* of power [69]. Since there is much experience in operating CNs, the administrative processes are well established, and billing and ownership structures are clear [69].

The lower flexibility connected to the CN design is the cause of various weaknesses. In CNs, it is more challenging to respond to the demand changes of the consumers, and the anticipation for network expansion requires over dimensioning components [23]. Implementing multiple renewable energy sources is more difficult due to the single generation point of CNs. The design principle of peak load generators in CNs generally causes inefficient use [69]. Furthermore, redundancy at a central level is generally required. Thus, unused or rarely used pumping and generation infrastructure is generally tied to the design [23]. A separated heat central in CNs requires an inefficient single-purpose use of building space for heating [58].

4.1.3. Comparison

The prosumer networks are rated in relation to conventional networks for each aspect listed in Table 1. If the prosumer network is expected to perform better in the considered aspect, “+” is used; if it is expected to be weaker in the considered aspect, “-“ is attributed. If a relatively small performance difference to PNs is expected, a “0” is assigned to the conventional network. If the performance difference is expected to be relatively large, the CN is categorized as either “-“ or “+”. The distinguishing factor shortly describes the reason for the predicted difference in performance. The summary is shown in Table 1

Table 1: Relative comparison of strengths and weaknesses of CNs and PNs;
 CN:“0” and PN:“+“ or “-“ for minor differences; CN:“+“ or “-“ and PN: “+“ or “-“ for greater differences

Aspect	CN	PN	Distinguishing factor
Combined heating and cooling	-	+	Number of pipelines needed
Flexibility	-	+	Number of generation and supply options
Robustness to condition changes	0	+	Impact of changing heat or temperature demand of participants
Redundancy	0	+	Over dimensioning of CN heat generators and unused pumping infrastructure
Control complexity	+	-	Number of data points/actuators, operation states, and optimization parameters
Space efficiency	0	+	Overall built space needed for installations due to single-purpose heat centrals
Maintenance effort	+	-	Number of points of failure and actuators, frequency of changing operation state
Billing complexity	0	-	Number of cost parameters and monitoring units
Investment costs	0	-	Cost of main network components
Exergy losses	0	-	Number of heat exchangers between a heat source and sink
Thermal losses	0	+	Amount of transported heat, shorter transportation distance
Integration of renewables or waste heat	-	+	Number of possibilities for the integration of decentral heat sources
Fuel demand	-	+	Generation efficiency, reduced losses, utilization of multiple heat sources
Part load efficiency	0	+	Potential for optimizing the operation point of pumps and generators in PNs
Pumping energy	0	+	Reduced transported mass flow

From the qualitative investigations on strengths and weaknesses, four main hypotheses for the performance comparison of PNs and CNs were deducted:

1. PNs are generally more flexible than CNs due to the increased number of heat sources and supply options.
2. PNs are generally more energy efficient than CNs due to the reduced heat losses in the network as well as the higher potential for utilizing waste heat and for operating the pumps and heat generators at their highest efficiency in part-load situations.
3. PNs generally require higher operation and control efforts than CNs due to the increased number of actuators and multiple modes of operation.
4. PNs generally cause higher capital- and operation-related costs than CNs due to their more complex substations, frequent changes of operation states, and the high number of actuators with moving parts.

The validity of these hypotheses depends on individual boundary conditions, but they still indicate the expected relative performance of the two network types.

4.2. Economic sensitivities

Nussbaumer et al. investigated the economic sensitivity of CNs to various influencing factors and the resulting impact on the economic efficiency of CNs [70]. The study results were used as a basis for a qualitative comparison of the sensitivities listed in Table 2. From the findings in [70], three economic impact and sensitivity categories were derived. “Very High”, “High”, and “Low” for the economic impact. Furthermore, “very sensitive” (“- -”), “Sensitive” (“-“), and “not very sensitive” (“0”) are used for ranking the sensitivity. The general comparison of strengths and weaknesses for CNs and PNs, outlined in subsection 4.1, is the basis for the qualitative sensitivity assessment. The distinguishing factor in Table 2 shortly describes the reason for the predicted difference in sensitivity between the CN and the PN.

Table 2: Influencing factors on economic efficiency and the sensitivity of CNs and PNs
 “- -” Very sensitive, “-“ sensitive, “0” not very sensitive

Influencing factor	Economic impact	Sensitivity		Distinguishing factor
		CN	PN	
Pipe diameter	Very High	- -	-	Reduced mass flow in PN pipelines
Pipe insulation	Low	-	0	Reduced mass flow in PN pipelines
Interest rate	High	-	- -	Higher investment cost in PN
Electricity price	Low	-	0	Reduced mass flow in PN pipelines
Fuel price	Very High	- -	-	Higher energy efficiency and reduced losses in PN
Temperature difference supply and return	High	- -	-	Reduced mass flow in PN pipelines
Full-load hours and heat density	High	-	- -	High investment costs in PN require cost reduction in heat production
Load Difference between summer and winter	Low	-	0	Multiple sources at different powers available in PN
Availability of waste heat/renewable energies	Very High	-	- -	High investment costs in PN require a reduction of heat cost
Network length and connection load	High	- -	-	Decentral production in PN is more flexible in adjustments of power and pipe diameter

The most relevant distinguishing factors for the sensitivities of the network types are the lower mass flow in PNs due to a partial direct consumption by prosumers, the higher investment costs for PNs, the structure of PNs allowing to address changing conditions more flexibly, and the hypothesized higher energy efficiency of PNs. Thus, the most relevant influencing factors for comparing CNs and PNs are pipe diameter, interest rate, fuel price, full-load hours, availability of renewable energies, and network length. These factors should be prioritized in an economic sensitivity analysis between CNs and PNs.

5. Adaptation of planning methods

Starting from this chapter, the thesis is focused on the most extreme form of prosumer integration in thermal networks: The PBN, which is comprised only of prosumers without any dominating central unit. Decentral actuators (pumps and control valves) in the substations enable bidirectional mass and energy flows in the hot and cold subnetworks for load-balancing between prosumers, as described by Lickleder et al. [41]. An experimental setup for PBNs is implemented in the CoSES laboratory at the Technical University of Munich [61]. Figure 3 shows the structure for a line PBN and a prosumer substation. This structure forms the scope for the dimensioning procedures proposed in this thesis.

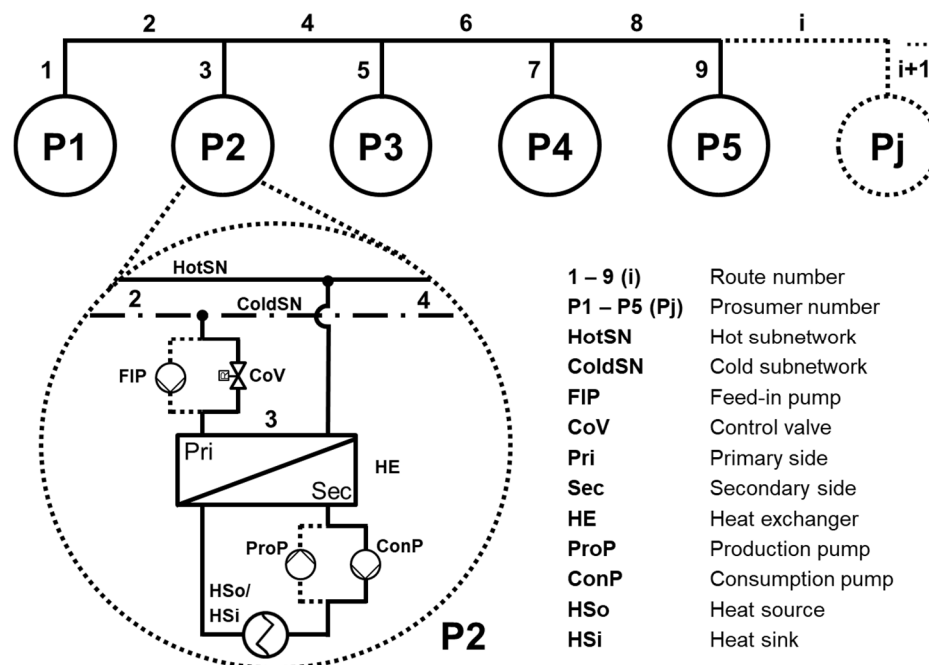


Figure 3: Structure and nomenclature of a line prosumer-based network

The feed-in pump (FIP) and control valve (CoV) are the decentral actuators that influence the pressure and mass flow on the primary network side, while the production pump (ProP) and the consumption pump (ConP) control the mass flow on the secondary side. When the prosumer is in production mode, FIP and ProP are active; CoV is closed, and ConP is inactive. In consumption mode, FIP and ProP are inactive, while CoV is open and ConP is active. In the scope of this thesis, two design premises regarding the exchange flexibility between the prosumers are considered:

1. All-Neighbor-Exchange (ANE): Each prosumer can exchange energy with each of the other prosumers in the network.
2. One-Neighbor-Exchange (ONE): Each prosumer can only exchange energy with directly neighboring prosumers.

5.1. Dimensioning approach

The design power flow is the basis for thermal dimensioning procedures [23]. Due to the hydraulic flexibility of PBNs, described in subsection 2.2 and depicted in Figure 1, the design power in the network components depends on other prosumers. Consequently, determining the significant power flows and, thus, the relevant dimensioning states is the preliminary stage for component design in line PBNs. In Figure 4, the proposed algorithm to determine the design power flows \dot{Q}_{max}^i in the distribution pipes (in *I*) and connection pipes (in *II*) is depicted. In this case, the process for the design premise ANE is shown. The process for ONE is similar but reduced to only consider energy exchange between directly neighboring prosumers. The pseudo-codes for both premises are included in appendix B. The network structure and nomenclature for line PBNs (see Figure 3) are the basis for the algorithm shown in Figure 4.

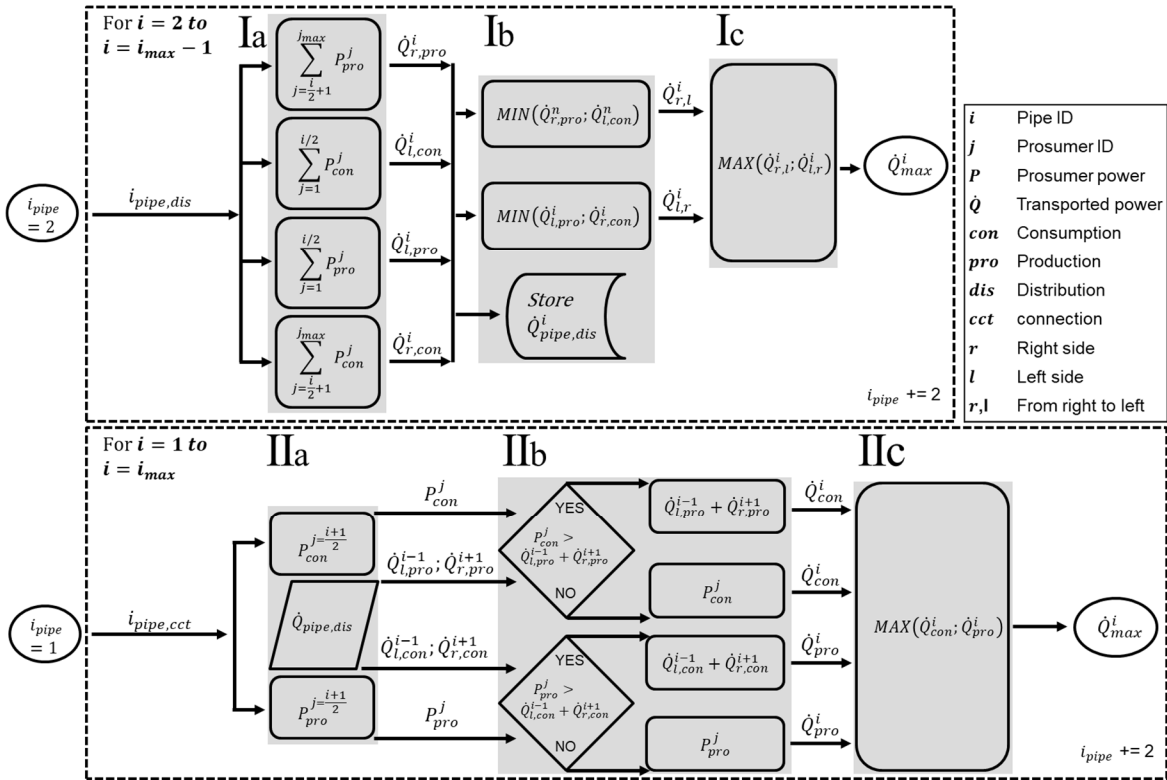


Figure 4: Algorithm for determining the design power flow for network pipes in line PBNs

The algorithm describes three main steps to determine the maximum power flow through the distribution and connection pipes of a line PBN. In *Step Ia*, the network is split into a right and left side, relative to the considered distribution pipe. Additionally, the total available demand ($\sum P_{con}^j$) and supply ($\sum P_{pro}^j$) power of prosumers on both network sides are determined. The power flow in the distribution pipe is characterized by the energy exchange

from the left to the right side and vice versa. Thus, in *Step Ib*, the two maximal power exchanges between the two sides are determined. Furthermore, the available demand and supply powers from *Step Ia* are stored for later use. Finally, in *Step Ic*, the bigger of the two possible power exchanges ($\dot{Q}_{r,l}^i$ and $\dot{Q}_{l,r}^i$) is calculated to result in the design power flow \dot{Q}_{max}^i for the distribution pipe. This process is repeated for all distribution pipes.

In the second part of the algorithm (*II*), the maximal power flow for the connection pipes to the prosumers is determined. Therefore, in *Step IIa*, the production and consumption power of the connected prosumer and the stored demand and supply power of the two neighboring distribution pipes (from *Step Ib*) are gathered. In *Step IIb*, the demand or supply power of the prosumer is compared to the available supply or demand in the rest of the network. If the prosumer demand or supply exceeds the available supply or demand, the power flow is limited to the power in the remaining network; otherwise, the prosumer characteristics describe the power conditions in the connection pipe. Finally, in *Step IIc*, the larger value between consumption and production power describes the design power flow \dot{Q}_{max}^i for the connection pipe. This process is repeated for all connection pipes.

The principles for hydraulic component dimensioning from conventional networks (see subsection 2.1) are applied to the main components in PBNs. However, the operation flexibility necessitates the consideration of the different exchange possibilities to determine the design conditions. The implementation of the component dimensioning for PBNs is described in detail in the following subsection, which is focused on the dimensioning tool.

5.2. Dimensioning tool for line prosumer-based networks

A tool for dimensioning line PBNs was built in Excel to partially automate the design process. It functions with a combination of formulas integrated directly into spreadsheets and macros executed with VBA macros. The structure, handling, and dimensioning steps of the dimensioning tool are described in this subsection. Additionally, a “read me” section in the tool describes the interaction for a user. The attached version of the tool includes the relevant inputs used for the investigations in this thesis. A cleaner version is available at: https://github.com/FabianSpeer/PBN_Dimensioning_Tool

5.2.1. Conditions and assumptions

First, the medium in the network pipes must be set to define the relevant physical properties. The density ρ in kg/m^3 , the kinematic viscosity ν in m^2/s and the specific heat capacity

c_p in $kJ/(kg \cdot K)$ of the medium at different temperatures are relevant for the calculation. These properties are included in the dimensioning tool in increments of $5 K$ from $-20 \text{ }^\circ\text{C}$ to $80 \text{ }^\circ\text{C}$. The properties for the energy carriers water and glycol-mixtures at concentration levels of 23% , 29% , and 35% are implemented.

The proposed method from 5.1 requires specifications on the prosumer characteristics, the limits of flow velocity and pressure gradient in the network pipes, and the targeted valve authorities. These specifications are parameters in the dimensioning tool and are set by the user. The needed inputs for the prosumers are the designed thermal consumption and production power P_{con} and P_{pro} of the prosumer in kW , the design temperature of return and supply on the secondary side $\vartheta_{cold}^{sec,pro}$ and $\vartheta_{hot}^{sec,con}$ in $^\circ\text{C}$, and the pressure drop in the primary side of the heat exchanger Δp_{HE} during design conditions. The prosumers in a line configuration are assigned unique IDs following the nomenclature shown in Figure 3.

In the next step, the properties of the piping must be defined. That includes the pipe roughness ε in mm , the available increments of the nominal size (DN), and the resulting inner diameters d_i of the piping. These increments vary between different piping types and manufacturers. In the tool, a plastic jacket pipe (PJP), an insulated steel pipe with a plastic casing from ISOPLUS [71], and uninsulated PE pipes from FRANK [72] are available. Then, the length of each piping section must be set following the structure depicted in Figure 3. Furthermore, it must be decided whether the pressure drop in individual resistors Δp_{ir} , from miscellaneous fittings is calculated separately with ζ -values, or a percentual approach is used. In early design stages, a percentual value between $10\text{-}20 \%$ of the pipe losses is recommended by Nussbaumer et al. [23]. Lastly, the maximum acceptable flow velocity u_{max} in m/s and pressure gradient R_{max} in pa/m for the connection and distribution pipes and the design temperature of the cold and the hot subnetwork $\vartheta_{cold,tar}^{prim}$ and $\vartheta_{hot,tar}^{prim}$ in $^\circ\text{C}$ must be set. For the dimensioning of the CoVs the targeted valve authority a_{tar}^{CoV} must be specified. For all assumptions, the numbering scheme of Figure 3 must be considered for the tool to function correctly. The required assumptions and the parameters used in the case study are summarized in Table 3.

5.2.2. Component Dimensioning

With the conditions and assumptions set by the user, the algorithm depicted in Figure 4 is applied to receive relevant power flows in all network pipes. This completes the information needed for component dimensioning. The main steps of the established methods described in subsection 2.1 are used to dimension the core network components according to the

different power flow conditions in PBNs. Figure 5 shows a flow chart of the dimensioning steps for each component, which are explained in more detail in the following section.

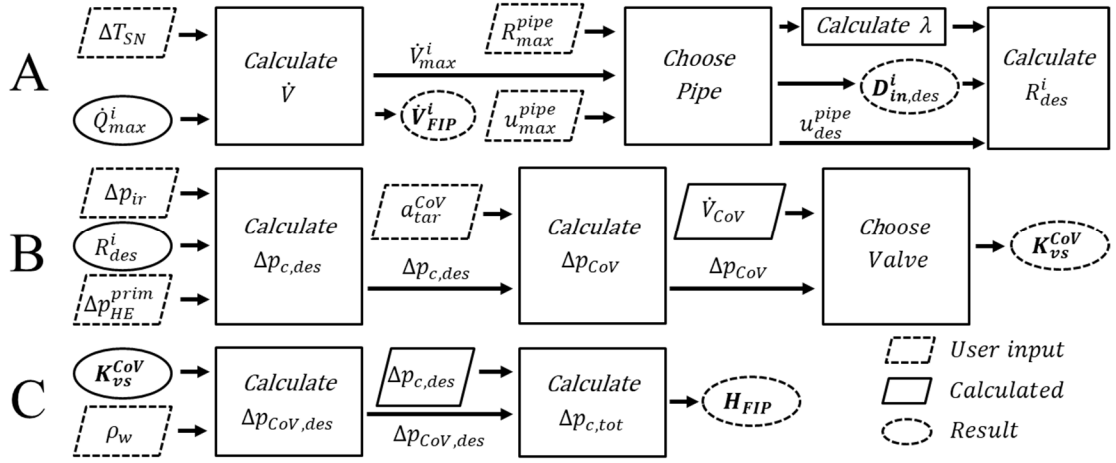


Figure 5: Flow chart for component design in the dimensioning tool

A: Dimensioning the network pipes

First, with the maximum power \dot{Q}_{max}^i transported through each network pipe and the targeted temperature difference between the subnetworks (SN) ΔT_{SN} , the maximum volumetric flow rate \dot{V}_{max}^i in m^3/h is calculated using this equation:

$$\dot{V}_{max} = \frac{\dot{Q}_{max}}{c_p * \Delta T} \quad (1)$$

With equation (2), a theoretical inner diameter that causes the specified maximum flow velocity u_{max}^{pipe} for each pipe is calculated:

$$d_i = 2 * \sqrt{\frac{\dot{V}_{max}}{\pi * u_{max}}} \quad (2)$$

The theoretical flow velocity at the determined pipe diameter d_i from equation (2) is calculated with equation (3):

$$u = \frac{4 * \dot{V}_{max}}{\left(\frac{d_i}{1000}\right)^2 * \pi} \quad (3)$$

The tool automatically chooses the next higher available pipe diameter following the previously defined pipe diameters from the manufacturer data sheets. Then, the resulting pressure gradient R is calculated with equation (4):

$$R = \frac{\lambda * \rho * u_{real}^2}{2 * \frac{d_{i,real}}{1000}} \quad (4)$$

To determine the friction factor λ used in equation (4), the value of the Reynolds number Re must first be determined with equation (5):

$$Re = \frac{d_{i,real} * u_{real}}{1000 * \nu} \quad (5)$$

If $Re < 2300$, equation (6) for laminar flow is used to calculate λ [73].

$$\lambda = \frac{64}{Re} \quad (6)$$

If $Re > 2300$, the explicit approximation of Colebrook's friction factor equation (7) from [74] is used to calculate the friction factor λ for hydraulically rough pipes:

$$\lambda = \left[\frac{1}{-2 \log_{10} \left(0,27 * \frac{\varepsilon}{D_i} - \frac{5,02}{Re} * \log_{10} \left(0,27 * \frac{\varepsilon}{D_i} + \frac{13}{Re} \right) \right)} \right]^2 \quad (7)$$

For the calculated pressure gradient R from equation (4), it is checked if $R \leq R_{max}$. If that is not the case, the next larger available pipe diameter is chosen by the tool until the condition is met. Then, the actual flow velocity u_{real} and pressure gradient R_{real} is calculated with equation (3) and equation (4) using the $d_{i,real}$ of the chosen pipe.

B: Dimensioning the control valves

With the previously set length of the pipe sections and the pressure gradient R_{real}^i the pressure drop of the pipes Δp_p is calculated, then, depending on the chosen approach, the pressure drop of the individual resistors Δp_{ir} is calculated with ζ -values or with a percentage of Δp_p . The pressure drop in the heat exchanger Δp_{HE} was set by the user. Subsequently, the pressure drop Δp_c in all possible hydraulic circuits (see Figure 1), is calculated with equation (8).

$$\Delta p_c = \Delta p_p + \Delta p_{ir} + \Delta p_{HE} \quad (8)$$

With the flow-dependent pressure drop in the hydraulic circuits known, the control valves can be dimensioned. The hydraulic circuit with the highest pressure drop is the relevant design hydraulic circuit (DHC). The targeted valve authority a_{tar}^{cov} , set by the user, determines the size of the control valve. According to Nussbaumer et al., the targeted valve authority should be between $0.2 - 0.3$, and the valve authority for the client in the hydraulically worst position should be $0.3 - 0.5$ [23]. Since the client in the hydraulically worst

position changes in PBNs, a conservative target value of 0.5 for the valve authority is recommended in PBNs. The valve authority a^{CoV} is defined by equation (9):

$$a^{CoV} = \frac{\Delta p_{CoV}}{\Delta p_{CoV} + \Delta p_c} \quad (9)$$

By combining equations (8) and (9), the pressure drop of the valve is calculated with equation (10). The hydraulic circuit with the most significant pressure loss determined with equation (8) is relevant in equation (10):

$$\Delta p_{CoV} = \frac{(\Delta p_p + \Delta p_{ir} + \Delta p_{HE})}{\left(\frac{1}{a^{CoV}} - 1\right)} \quad (10)$$

Next, the theoretical flow coefficient (K_{vs} -value) of the control valve is calculated with equation (11) from the DIN EN 60 534. The relevant flow rate \dot{V} is derived from the determined consumption power flow \dot{Q}_{con}^i in the prosumer connection pipe in Figure 4.

$$K_v = \dot{V} * \sqrt{\frac{\rho}{1000 * \frac{\Delta p_{CoV}}{100}}} \quad (11)$$

The K_v -value is calculated for the control valve of each prosumer. A real-world control valve is chosen with the next larger K_{vs} -value to not exceed a valve authority of 0.5 and, consequently, limit the pressure losses. Thus, the actual pressure loss in the chosen CoV $\Delta p_{CoV,real}$ is calculated with equation (12):

$$\Delta p_{CoV} = \left(\frac{\dot{V}}{K_{vs}}\right)^2 * 100 \quad (12)$$

C: Dimensioning the feed-in pumps

For the FIP, the relevant dimensioning values are the volumetric flow \dot{V}_{FIP} and the pump head H_{FIP} during design conditions. The relevant \dot{V}_{FIP} for the FIP is derived from the determined production power flow \dot{Q}_{pro}^i in the prosumer connection pipe in Figure 4. For each FIP, the needed head for all possible hydraulic circuits is calculated with equation (13). The largest pump head calculated with equation (13) is used for pump dimensioning.

$$H_{FIP} = \Delta p_p + \Delta p_{ir} + \Delta p_{HE} + \Delta p_{CoV} \quad (13)$$

Due to the influence of the pressure drop in CoVs, the DHC for FIPs might differ from the DHC that was relevant for designing the CoVs. Based on the dimensioning results, the tool attached to this thesis summarizes the suggested inputs for the ProsNet [49] models of up to five prosumers in Dymola.

With the methods described in this section, the core network components of line PBNs can be dimensioned for the comparative case study in the following chapters.

6. Dimensioning the case study networks

The characteristics of the residential houses emulated in the CoSES-lab [61] are used to dimension the CN and PN case study networks. The dimensioning tool and methods described in section 5 are used to size the network components for the PBN. Established design methods (see subsection 2.1) and, consequently, the formulas described in subsection 5.2 are applied to design the CN.

6.1. Network characteristics

The assumptions for the relevant boundary conditions and network parameters used to dimension the PBN with the dimensioning tool are listed in Table 3.

Table 3: Network parameters used for dimensioning the case study

Description	Symbol	Value	Unit
Medium in the network pipes	-	Water	–
Type of network pipes	-	Plastic jacket pipes	–
Absolute pipe roughness	ε	0.02 [75]	mm
Length of the route sections	l_{route}	see Table 4	m
Maximum flow velocity in connection pipes	$u_{max}^{pipe,cct}$	1 [70]	m/s
Maximum flow velocity in distribution pipes	$u_{max}^{pipe,dis}$	1.5 [70]	m/s
Maximum pressure gradient in connection pipes	$R_{max}^{pipe,cct}$	250 [23]	Pa/m
Maximum pressure gradient in distribution pipes	$R_{max}^{pipe,dis}$	250 [23]	Pa/m
Target temperature in the hot subnetwork	$\vartheta_{hot,tar}^{prim}$	65	°C
Target temperature in the cold subnetwork	$\vartheta_{cold,tar}^{prim}$	50	°C
Targeted valve authority	a_{tar}^{CoV}	0.5 [23]	–
Pressure gradient in individual resistors (e.g., fittings)	R_{ir}	10 [23]	%
Maximal prosumer consumption power	$P_{max}^{pros,con}$	see Table 5	kW
Maximal prosumer production power	$P_{max}^{pros,pro}$	see Table 5	kW
Target secondary supply temperature consumption mode	$\vartheta_{hot,tar}^{sec,con}$	60	°C
Set secondary return temperature in consumption mode	$\vartheta_{cold,set}^{sec,con}$	45	°C
Pressure loss through heat exchangers in design conditions	Δp_{HE}^{prim}	20	kPa
Design temperature difference in the heat exchangers	ΔT_{HE}	3	K

In Table 4, the lengths of the network sections are listed. The values resulted from scaling the network configuration emulated in the CoSES-lab to a small-scale, local PBN. [76] For the CN, a distance of 40 m for the connection of the heat central was assumed.

Table 4: Length of network routes in the conventional and prosumer-based network

Network section no.	0	1	2	3	4	5	6	7	8	9
Length CN [m]	40	10	40	10	40	10	49.5	10	46.5	10
Length PBN [m]	0	10	40	10	40	10	49.5	10	46.5	10

6.2. Prosumer characteristics

Due to the proposed early-stage application of the dimensioning method, the CoSES example houses are categorized into TABULA [77] building typologies to determine their heat demands. A detailed calculation or simulation of secondary side heat demands and a detailed dimensioning of heat generators lies outside of the scope of this thesis. For the SH power demand, ventilation and transmission losses of the houses were calculated according to the simplified procedure of the *DIN EN 12831-1* for the climate in Munich, using the respective heat transfer coefficients stated in the TABULA typologies assigned in Table 5. For the DHW power demand, the peak flows were determined according to the *DIN 1988-300*. The required additional power was calculated for temperatures described in *DIN 12831-3 A100*. A DHW storage with a discharge time of *10 min (DIN 4708-1)* and a recharge time of *60 min* was assumed. All prosumers are equipped with heat sources capable of generating *100 %* of their total heat demand, as suggested in [78]. Their properties and resulting demands are listed in Table 5.

Table 5: Prosumer characteristics applied in the case study

	Pros1	Pros2	Pros3	Pros4	Pros5
CoSES name	SF1	SF3	SF4	MF5	SF2
Living Area [m²]	300	400	300	750	300
No. of Apartments	1	3	2	4	2
Age Class	1995 - 2002	From 2016	2007 – 2009	1995 – 2002	2007 - 2009
TABULA Code	SFH.09.Gen	SFH.12.Gen	SFH.10.Gen	MFH.09.Gen	SFH.10.Gen
TABULA Standard	Improved	Improved	Improved	Improved	Improved
Heat loss transmission [kW]	13.0	9.9	8.9	16.7	8.9
Heat loss ventilation [kW]	5.2	1.1	4.3	13.0	4.3
Heat demand DHW [kW]	7.1	10.5	8.1	12.2	8.1
Total heat demand [kW]	25.3	21.5	21.2	41.8	21.2

6.3. Component dimensioning

In this section, the resulting component dimensions for the PBN and CN are summarized. Since the same boundary conditions are relevant for heat exchangers in both network types, the same heat exchangers are used for the CN and PBN. The heat exchangers from

SWEP [79] were dimensioned with *DThermX* [80] for the conditions in the substations specified in the previous subsections. The results are listed in Table 6.

Table 6: Heat exchanger dimensions in the PBN and the CN

Prosumer No.	Type	\dot{Q}_{max}^{HE} [kW]	\dot{m}_{des}^{HE} [m ³ /h]	$\Delta p_{HE,des}$ [kPa]	$\Delta p_{HE,real}$ [kPa]
1	B15Tx26	25.27	0.40	20	19.9
2	B15Tx24	21.51	0.34	20	17.0
3	B15Tx24	21.24	0.34	20	16.7
4	B15Tx44	41.83	0.67	20	20.9
5	B15Tx24	21.24	0.34	20	16.7

The manufacturer product lines for the network pipes and the control valves are included in the dimensioning tool and automatically dimensioned, as described in Chapter 5. The primary side pumps are dimensioned with the Grundfos online product center [81].

6.3.1. Prosumer-based network

The product lines used to dimension the PBN components are listed in Table 7.

Table 7: Manufacturers and product lines used in the PBN case study

Component	Manufacturer	Product line
Pipes	ISOPlus [71]	Plastic jacket pipes (standard)
Control valves	Sauter [82]	VUN
Circulation pumps	Grundfos [83]	CR – inline pumps
Heat exchanger	SWEP [79]	B15T

In Table 8 to Table 10, the component dimensions and the relevant design values output by the dimensioning tool for the PBN are listed.

Table 8: Pipe dimensions and designed power and volume flows in the PBN

Pipe No.	DN	$d_{t,des}^{pipe}$ [mm]	u_{des}^{pipe} [m/s]	l_{route} [m]	R_{des}^{pipe} [Pa/m]	\dot{Q}_{max}^i [kW]	\dot{V}_{max}^i [m ³ /h]
1	25	27.3	0.70	10	215.51	25.27	1.47
2	25	27.3	0.70	40	215.51	25.27	1.47
3	25	27.3	0.59	10	160.58	21.51	1.25
4	32	36	0.74	40	171.35	46.78	2.72
5	25	27.3	0.59	10	157.03	21.24	1.24
6	40	41.9	0.74	49.5	140.80	63.07	3.67
7	32	36	0.66	10	139.58	41.83	2.44
8	25	27.3	0.59	46.5	157.03	21.24	1.24
9	25	27.3	0.59	10	157.03	21.24	1.24

Table 9: Control valve dimensions and designed operating points in the PBN

Prosumer No.	Type	\dot{V}_{des}^{CoV} [m³/h]	$\Delta p_{CoV,des}$ [kPa]	K_{ps}^{CoV} [m³/h]	a_{des}^{CoV} [-]
1	VUN015F320	1.47	83.36	1.6	0.42
2	VUN015F320	1.25	60.37	1.6	0.39
3	VUN015F320	1.24	58.91	1.6	0.41
4	VUN015F310	2.44	93.53	2.5	0.48
5	VUN015F320	1.24	58.91	1.6	0.34

Table 10: Pump dimensions and designed operating points in the PBN

Prosumer No.	Type	\dot{V}_{des}^{CenP} [m³/h]	H_{des}^{CenP} [mH ₂ O]	H_{des}^{CenP} [kPa]
1	CR 1-7 A-A-A-E-HQQE	1.47	19.45	190.72
2	CR 1-7 A-A-A-E-HQQE	1.25	17.39	170.54
3	CR 1-7 A-A-A-E-HQQE	1.24	16.89	165.60
4	CR 3-5 A-A-A-E-HQQE	2.44	18.41	180.55
5	CR 1-7 A-A-A-E-HQQE	1.24	20.09	197.00

6.3.2. Conventional network

Figure 6 shows a suggested minimum configuration of substation components in CNs. A combined differential and control valve is chosen for the configuration instead of a separate valve for differential pressure and volume flow control since it is the recommended variant by various guides and planning handbooks. [23, 84, 85] For the pressure loss in the CN heat central, 30 kPa is assumed.

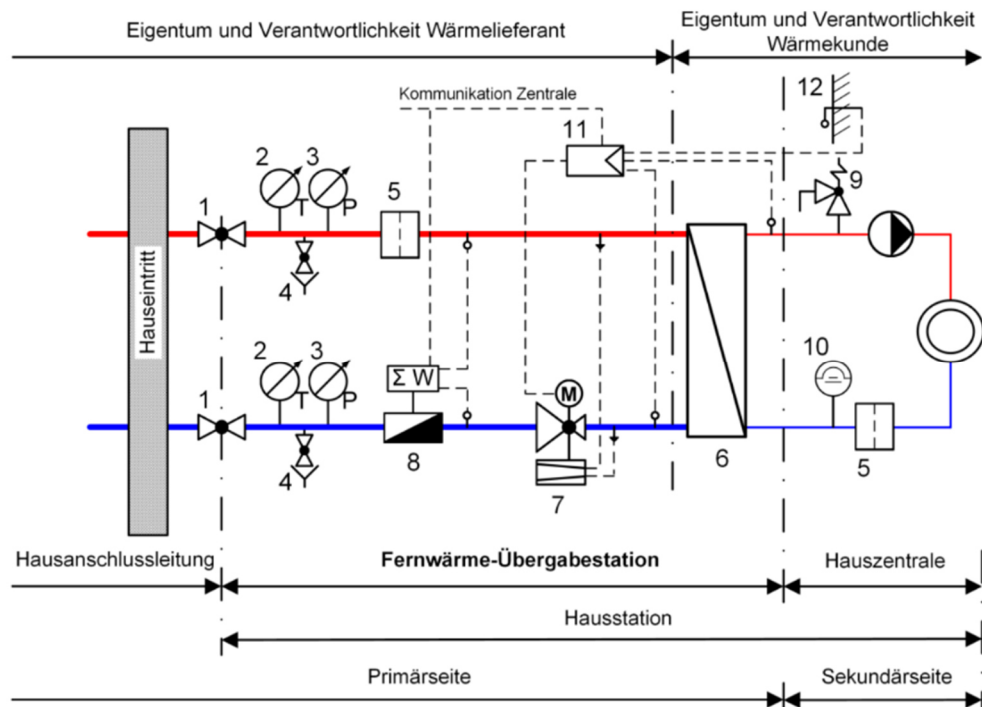


Figure 6: Recommended components for a CN substation [84]

The product lines used to dimension the CN components are listed in Table 11.

Table 11: Manufacturers and product lines used in the CN case study

Component	Manufacturer	Product line
Pipes	ISOPlus [71]	Plastic jacket pipes (standard)
Combined valves	Belimo [86]	EV..R2+BAC - Energy valve
Circulation pumps	Grundfos [83]	CR – inline pumps
Heat exchanger	SWEP [79]	B15T

In Table 12 to Table 14, the component dimensions and used design values for the CN are listed. The Belimo energy valves are dimensioned according to the planning guidelines provided by the manufacturer [87, 88].

Table 12: Pipe dimensions and designed power and volume flows in the CN

Pipe No.	DN	$d_{i,des}^{pipe}$ [mm]	u_{des}^{pipe} [m/s]	l_{route} [m]	R_{des}^{pipe} [Pa/m]	\dot{Q}_{max}^i [kW]	\dot{V}_{max}^i [m ³ /h]
0	50	53.9	0.93	40	148.9	131.10	7.63
1	25	27.3	0.70	10	204.5	25.27	1.47
2	50	53.9	0.75	40	101.0	105.82	6.16
3	25	27.3	0.59	10	153.2	21.51	1.25
4	40	41.9	0.99	40	226.6	84.32	4.91
5	25	27.3	0.59	10	149.9	21.24	1.24
6	40	41.9	0.74	49.5	134.0	63.07	3.67
7	32	36	0.66	10	133.1	41.83	2.44
8	25	27.3	0.59	46.5	149.9	21.24	1.24
9	25	27.3	0.59	10	149.9	21.24	1.24

Table 13: Belimo energy valve dimensions and designed operating points in the CN

Prosumer No.	Type	\dot{V}_{des}^{CoV} [m ³ /h]	$\Delta p_{CoV,des}$ [kPa]	$K_{vs,theo}^{CoV}$ [m ³ /h]	α_{des}^{CoV} [-]
1	EV020R2+BAC	1.47	9.40	4.8	-
2	EV020R2+BAC	1.25	6.81	4.8	-
3	EV020R2+BAC	1.24	6.64	4.8	-
4	EV025R2+BAC	2.44	9.04	8.1	-
5	EV020R2+BAC	1.24	6.64	4.8	-

Table 14: Pump dimensions and designed operating points in the CN

Description	Type	\dot{V}_{des}^{CenP} [m ³ /h]	H_{des}^{CenP} [mH ₂ O]	H_{des}^{CenP} [kPa]
Central plant	CR 10-3 A-A-A-E-HQQE	7.63	13.97	137.02

6.3.3. Comparison

The impact of the different structural principles for the CN and PBN component design becomes apparent when directly comparing the dimensions and design values of the core components. The chosen dimensions (DN) of the network pipes are depicted in Figure 7.

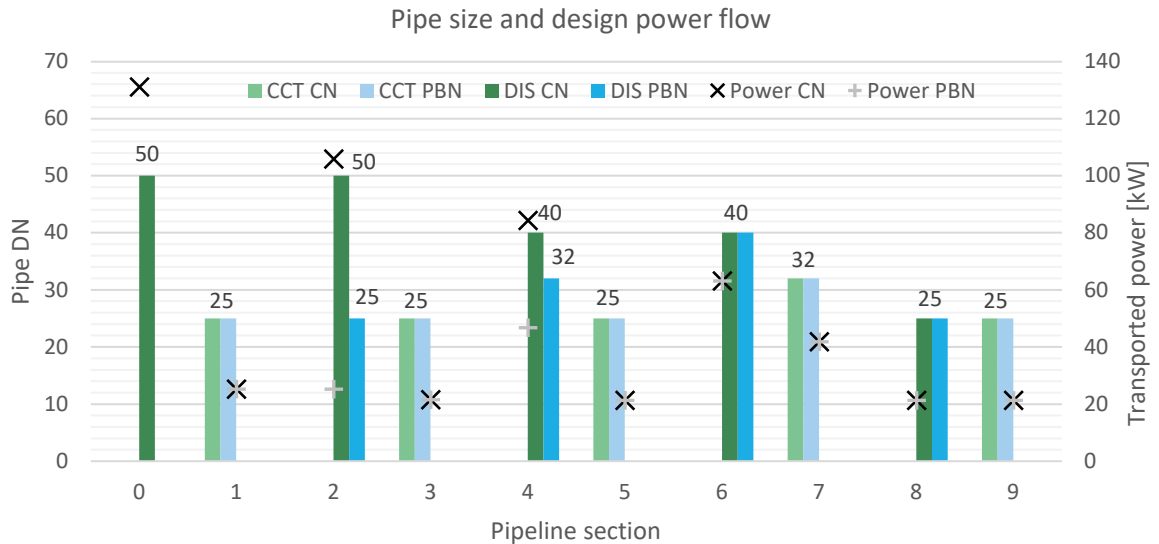


Figure 7: Sizes of the dimensioned piping sections in the PBN and CN

As shown in Figure 7, the CN requires larger pipe sizes for the distribution pipe sections 2 and 4. Additionally, an extra pipe section 0 is needed in the CN to connect the heat generators in the central plant to the network. Due to the structure of CNs, this additional pipe section needs to transport the most power and, thus, is typically the largest pipeline in the network. The nearly linear decrease of transported power in the CN distribution pipes (DIS CN) is visualized by the black crosses. In pipes 0, 2, and 4 (distribution pipes between heat central and Prosumer 3), the CN must transport more power than the PBN. In the remaining pipes, the transported power is equal. The dark green bars show the effect on the required pipe sizes. Consequently, an overall higher effort and costs for the piping network of the CN must be expected due to larger pipe sizes, longer routing, and potentially increased trench sizes.

Figure 8 compares the design pump heads for the primary side pumps in both networks.

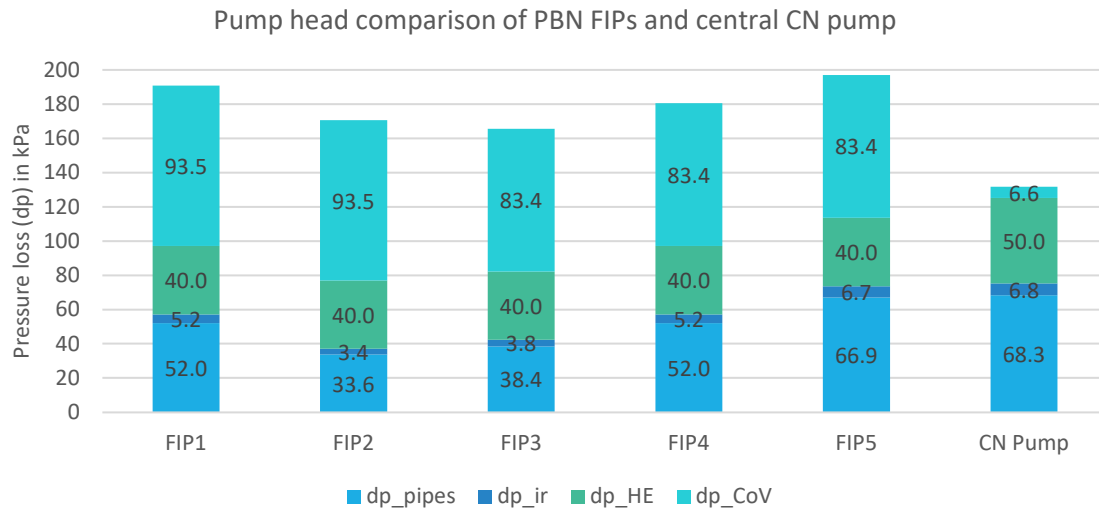


Figure 8: Dimensioned pump heads for the PBN FIPs and the central CN pump

Due to the line layout of the PBN, the distance to a potential consumer is smaller for FIPs in the middle of the network compared to FIPs on the edge of the network. Thus, FIP2, FIP3, and FIP4 require less head than FIP1 and FIP5 (see Figure 8). Consequently, if possible, the prosumer expected to supply the most heat to the grid should be located towards the middle of the network to minimize the required pumping energy. In the case of Prosumer 1 (FIP1), the effect of different DHCs (see subsection 5.2) for the primary side actuators can be observed. The pressure loss in pipes (dp_{pipes}) of 52.0 kPa shows that the DHC for the FIP is the connection to Prosumer 4 (Pros4). In contrast, the DHC for the CoV is the connection to Pros5 with a dp_{pipes} of 66.9 kPa . (see Table 8). This is due to the high pressure drop of the dimensioned real-world CoV at Pros4 compared to Pros5 (see Table 9).

In the case of the CN pump head, the significantly smaller pressure loss in the CoV stands out. This is explained by the design of the used pressure independent control valves. In contrast to traditional CoVs, these valves are not dimensioned for a particular valve authority. They require only small differential pressures to reach design volume flows. Since the valves automatically compensate for any rise in differential pressure above the required minimum, good control behavior is still ensured [87]. The assumed pressure drop of 30 kPa in the heat central of the CN is considered in the pressure loss in heat exchangers (dp_{HE}). Before comparing the economic efficiency of the two network variants, the functionality of the dimensioned PBN components is validated in the next chapter.

7. Tool validation - Dymola simulation

The properties from the components, dimensioned in Chapter 6, and the network conditions specified in Table 3 are implemented into a thermohydraulic grid model. The ProsNet [51] Modelica library was used to model the PBN. The model was built and simulated in Dymola, the Dassault Systèmes environment for the Modelica modeling language [89]. A section of the PBN model in Dymola, showing Pros4 and Pros5, is depicted in Figure 9.

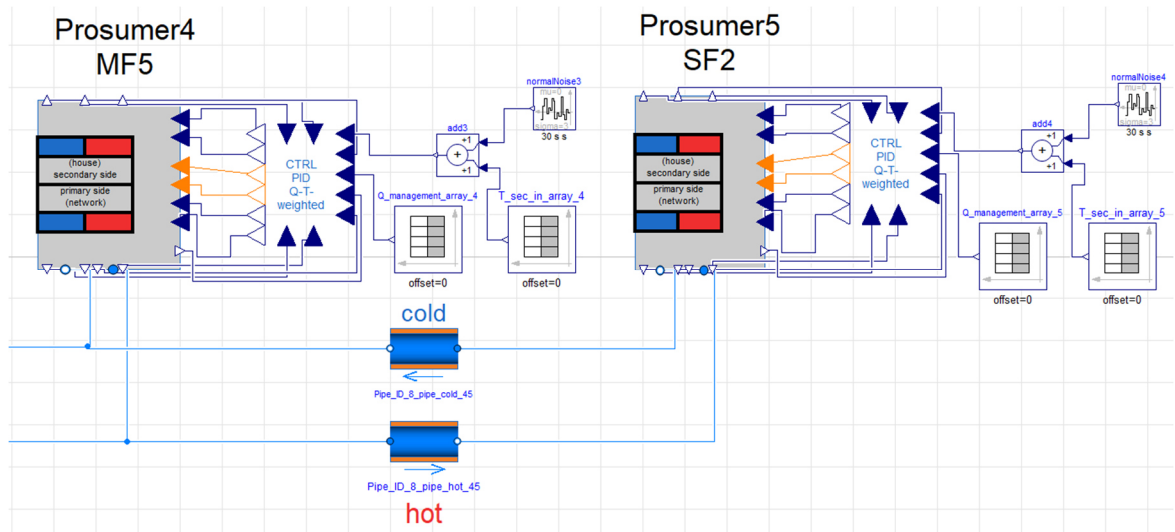


Figure 9: Section of the case study PBN model in Dymola

The functionality of the designed PBN components is assessed by analyzing the resulting thermohydraulic network states in the simulation. The accuracy of the proposed design method is assessed by comparing the design states predicted by the dimensioning tool and the operating states of the actuators and network pipes in the thermohydraulic simulation. Different energy exchange scenarios are manually specified for the simulation. The scenarios are chosen to observe the components' behavior during design and part load situations. The criteria for validation are:

1. Accuracy of the predicted design power flows in network pipes (\dot{Q}_{max}^i): comparison with maximal power flows during all exchange scenarios.
2. A sufficient supply of consumers regarding the transferred power (\dot{Q}_{con}^j) and secondary supply temperature (ϑ_{hot}^{sec}) during all load conditions.
3. Correct dimensioning of actuators: investigation of valve opening (κ_{set}^{CoV}), pump speed (u_{set}^{FIP}) and operating state $\Delta p(\dot{V})$ during design load conditions.

Since the control behavior of the decentral actuators is crucial for the functionality of PBNs, the pumps and control valves are dynamically controlled during the simulation by a

weighted PID control approach proposed by Lickleder et al. [54]. The control and target values for the four PID controllers, shortly described in subsection 2.2.3, and the applied weighting are summarized in Table 15. In principle, the error of the two target values is multiplied by their respective weight to adjust their ratio in a total error which is then input into the PID controller [54].

Table 15: Applied weighting for the target values of the four PID controllers [54] in all prosumers

Name	Control value	Target value 1	Weight 1	Target Value 2	Weight 2
PID1	u_{set}^{ConP}	\dot{Q}_{con}^j	0.4	ϑ_{hot}^{sec}	0.6
PID2	κ_{set}^{CoV}	\dot{Q}_{con}^j	0.9	ΔT_{prim}	0.1
PID3	u_{set}^{ProP}	\dot{Q}_{pro}^j	0.85	ΔT_{sec}	0.15
PID4	u_{set}^{FIP}	\dot{Q}_{pro}^j	0.85	ϑ_{hot}^{SN}	0.15

The weighting in Table 15 was chosen after manual tweaking, with the intent of minimizing the supply temperature and power transfer errors in all prosumers so that the heat demands of the prosumers in consumption mode are met. Overall, this dynamic control approach was chosen to assess if the control behavior of the dimensioned decentral actuators is suited for the dynamic load situations in the PBN at hand.

The thermal resistance in the pipes was set to $1000 (Km)/W$ to prohibit thermal losses. This was done because the manually set exchange scenarios (see subsection 7.1) cannot account for variable thermal losses. Thus, losses in the pipes would distort the results of the simulation. A 20 % dimensioning buffer was applied to the maximum secondary volume flow and nominal heat transfer of the heat exchangers. The secondary side pumps are modeled as ideal pumps. The chosen simulation parameters for the ProsNet [51] models and the PID controllers [54] are documented in the appendix (see Table C.2).

7.1. Exchange scenarios

The exchange scenarios (Sc) were chosen to put each prosumer at least once in a consumption design state and once in a production design state. Two criteria must be fulfilled for a prosumer to be in its design state. First, it must operate with maximum production or consumption power (see Table 5). Second, the transported power flow in the DHC for the FIP in production mode and DHC for the CoV in consumption mode is maximal, as defined by the algorithm in subsection 5.1. Figure 10 shows the qualitative pressure curves in the design scenarios Sc1 to Sc4, and the DHCs for the FIPs and CoVs are highlighted.

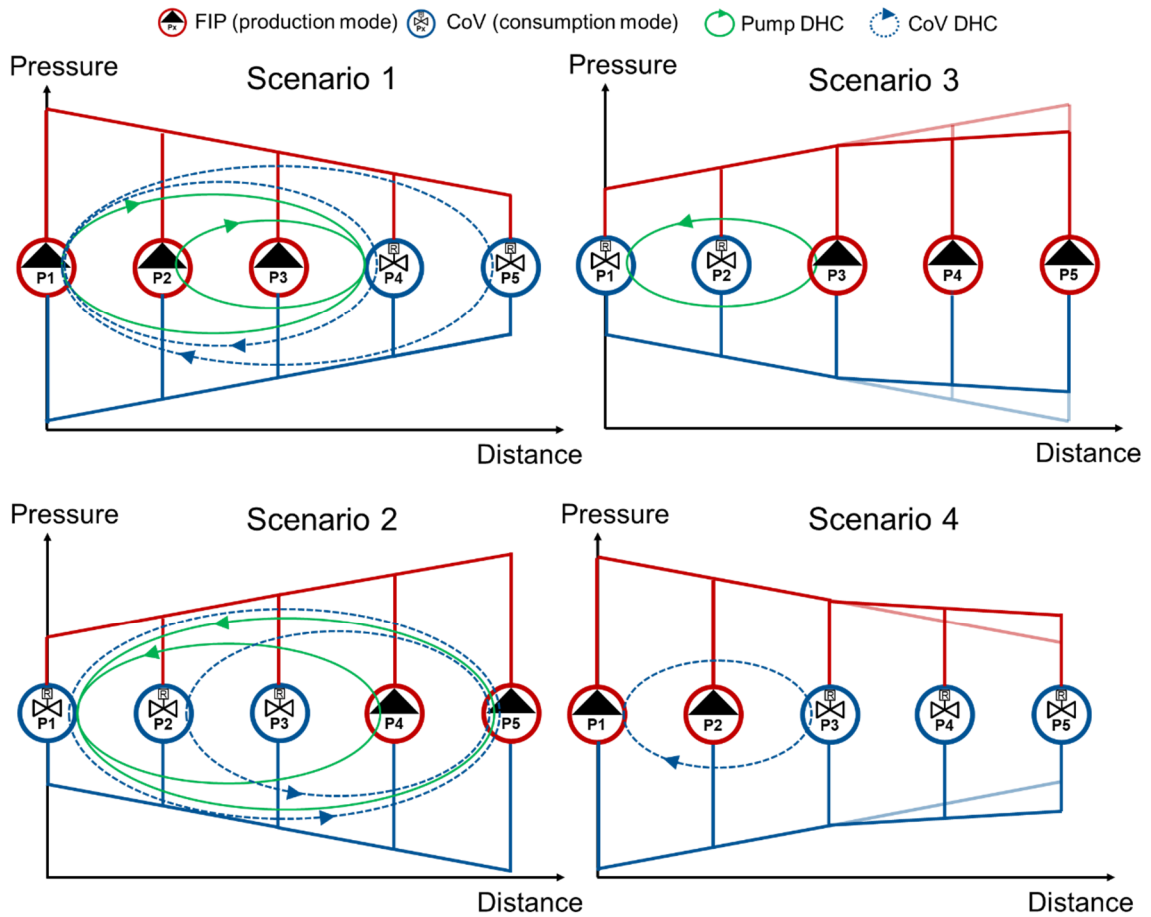


Figure 10: Qualitative pressure curves and DHCs for pumps and control valves in the exchange scenarios 1 to 4

In Sc1, the production design states for the FIP1 and FIP2 and the consumption design state for the CoV4 and CoV5 are observed. Pros3 is operating in part-load since the prosumer powers, set in Table 5, make it impossible for all prosumers to be in a design state simultaneously (see Figure 11). Consequently, a different scenario is required to achieve the design states for Pros3. The chosen design scenario Sc3 for the FIP3 is also shown in Figure 10, in which Pros1, Pros2, and Pros3 operate under maximum loads, while Pros4 and Pros5 must operate in part load (see Figure 11). Since the consumption power and the production power for all prosumers are assumed to be equal, the missing design states can be achieved by inverting the power flow of all prosumers during scenarios 1 and 3. Thus, the inverted production design scenario for the FIP of a prosumer results in the consumption design scenario relevant to the CoV of the same prosumer. The inverted Sc1 is named Sc2, and the inverted Sc3 describes Sc4.

The relevant design scenarios for all actuators are summarized in Table 16.

Table 16: Design scenarios for the actuators

Design scenario for:	Scenario 1		Scenario 2		Scenario 3		Scenario 4	
	FIP	1 & 2	FIP	4 & 5	FIP	3	FIP	-
CoV	4 & 5	CoV	1 & 2	CoV	-	CoV	3	

Additionally, the observation of the network behavior in part-load situations is desired. Thus, two additional scenarios (5 and 6) are chosen, corresponding to half the power flows of Sc1 and Sc2, respectively. The prosumer loads during the six described scenarios are depicted in Figure 11.

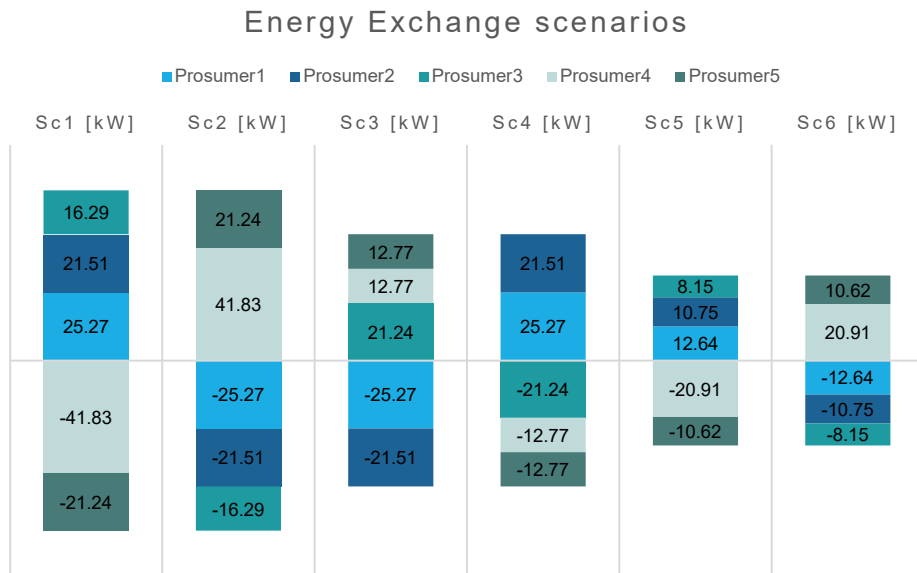


Figure 11: Prosumer load situations during the exchange scenarios

Each scenario is simulated for 1 hour with simulation steps of 10 seconds. Before and after each scenario, transition states with half the scenario's power are set for 15 minutes. The set timelines for the power management arrays of each prosumer (see Figure 9) are listed in the appendix (see Table C.1). For the temperature management arrays, each prosumer was attributed the values for $\vartheta_{hot,tar}^{sec,con}$ or $\vartheta_{cold,set}^{sec,con}$ specified in Table 3 for production mode and consumption mode, respectively.

7.2. Results

For evaluating the functionality of the dimensioning method, the steady-state conditions in network components during the defined exchange scenarios are relevant. Thus, the following values are read at the end of each 1-hour simulation section when the operation state has stabilized. The absolute errors for the maximum simulated power flows $\dot{Q}_{max,sim}^i$ and the maximum volume flow $\dot{V}_{max,sim}^i$ in the nine pipe sections are shown in Figure 12.

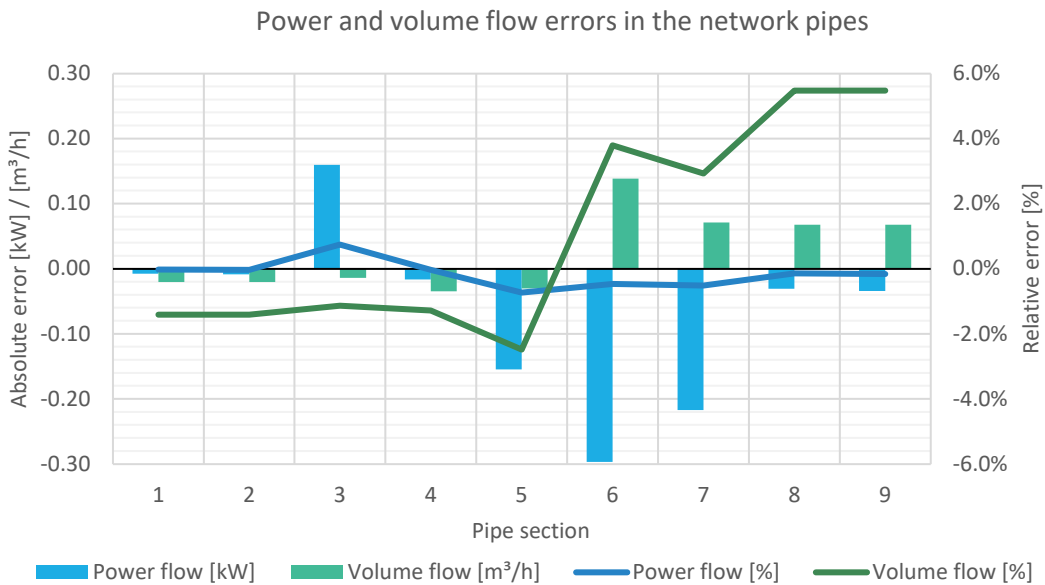


Figure 12: Absolute errors for simulated power and volume flow compared to design power and volume flow in the PBN network pipes

The maximal relative deviation for \dot{Q}_{max}^i is 0.7 % and occurs during Sc3. The small errors for \dot{Q}_{max}^i indicate that the algorithm presented in Figure 4 accurately predicts the design power flows in the network pipes. Thus, the first validation criterion is fulfilled. The maximal relative deviation for \dot{V}_{max}^i is 5.5 % and occurs in pipe sections 8 and 9 during Sc1. This increases the pressure gradient in the pipe compared to the design value. However, with the chosen pipe dimensions (see Table 8), the pressure gradient is still below the set maximum of 250 pa/m.

Figure 13 depicts the absolute errors for \dot{Q}_{con}^j and ϑ_{hot}^{sec} that resulted from the simulation of the prosumers during their design (des) scenario and during part load (pl) scenarios Sc5 and Sc6 as defined in subsection 7.1.

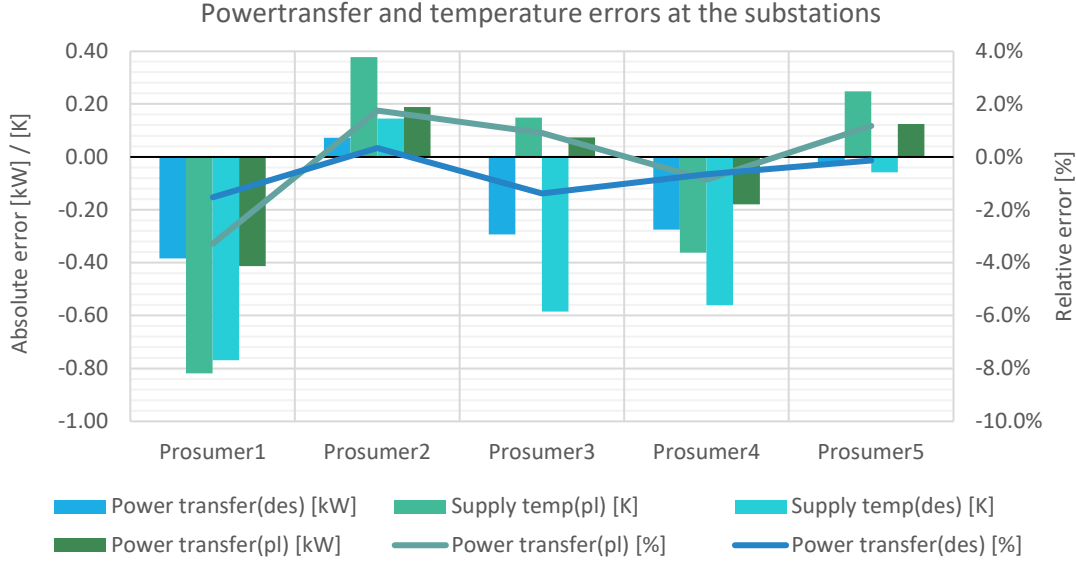


Figure 13: Errors for simulated and designed values for consumption power and secondary supply temperature during design and part load consumption scenarios

The maximal relative error for \dot{Q}_{con}^j is 1.5 % during design conditions in Sc2 and 3.3 % in the part-load Sc6. The maximal deviation of ϑ_{hot}^{sec} is $-0.77 K$ during design conditions in Sc4 and $-0.82 K$ in the part-load Sc6. With the small recorded errors, a sufficient supply of the connected prosumers with a setpoint supply temperature of $\vartheta_{hot}^{sec} = 60 \text{ }^\circ\text{C}$ can be assumed. Consequently, the consumption demands of all prosumers are met during every scenario. Thus, the second validation criterion is regarded as fulfilled.

The third criterion is focused on the actuator operating states. The operating states are defined by volume flow and the pressure difference in the actuator. Since the differential pressure and the volume flow depend on each other, a volume flow error also causes deviations from the designed differential pressure of the actuator. Volume flow errors were already recorded in the network pipes (see Figure 12). These deviations result from an error in the temperature spread ($\Delta T_{set}^{prim} = \vartheta_{hot,set}^{prim} - \vartheta_{cold,set}^{prim}$), since the power flows in the pipes matched the design nearly perfectly, and the values are connected by equation (14).

$$\dot{Q}_{des}^{pipe} = \rho * c_p * \dot{V} * \Delta T_{set}^{prim} \quad (14)$$

Where ρ and c_p can be considered quasi-constant physical properties of the medium in the relevant temperature ranges.

With the connection described in equation (14), the errors for ΔT_{set}^{prim} shown in Figure 14, directly cause deviations from the expected volume flow in the actuators.

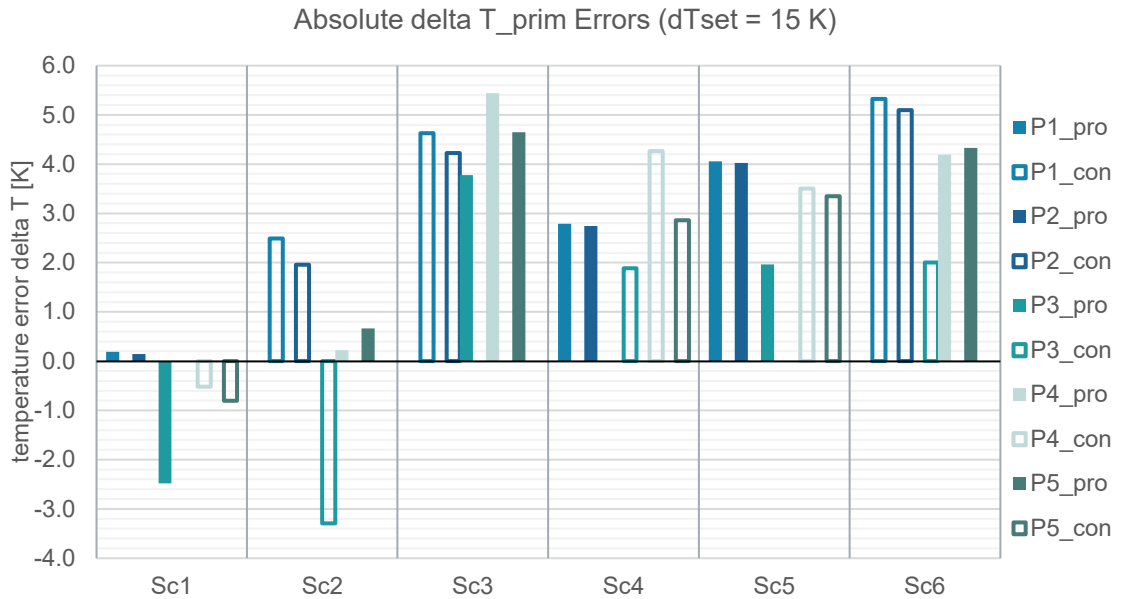


Figure 14: Absolute error for the primary side temperature spread across all scenarios

It is noticeable that the errors in Figure 14 are primarily positive and thus cause a reduced volume flow. The errors are at their lowest during scenarios 1 and 2 when the energy exchange in the network is the highest. A probable cause of the deviations is the weighting applied to the PID controllers (see Table 15), which prioritizes power flow and supply temperature over the temperature spread. Additionally, the weighted PID controller itself is still undergoing research. [54] Thus, the current structure of the controller could also cause or amplify the deviations.

Table 17 shows the normalized control values for the FIP speed and the CoV opening in a range from 0 to 1 during their respective design scenarios.

Table 17: Normalized speed of FIPs and opening of CoVs at their operating points

Normalized values	P1	P2	P3	P4	P5
u_{set}^{FIP} [0..1]	0.80	0.74	0.56	0.80	0.70
κ_{set}^{CoV} [0..1]	1.00	0.80	1.00	1.00	0.93

The u_{set}^{FIP} at the duty points of the pumps in Table 17 lie between 0.56 and 0.80. According to Jones et al., optimized pump duty points usually lie between 30-75 % of the total load [43]. Thus, the chosen pump sizes can be considered fitting for the PBN. The κ_{set}^{CoV} is 1 for the prosumers at the hydraulic worst point during their consumption design scenario (see Figure 10), as intended to minimize pressure losses. For Pros2 and Pros5, the CoV is

partially closed ($\kappa_{set}^{CoV} < 1$) to adjust to the pressure conditions created by the other prosumers in Sc1 and Sc2 (see Figure 10). Thus, the actuator control, in general, works as intended, but the errors in Figure 14 suggest that the current state of the controller (see Table 15) is causing deviations from the targeted conditions, especially during part-load situations.

In Figure 15, the operating points for each actuator dimensioned with the dimensioning tool are compared to the operating points resulting from the simulation of their design scenario (see Table 16). Additionally, the pump curves of the two used FIP types (see Table 10) at maximum speed (u_{max}^{FIP}) are displayed.

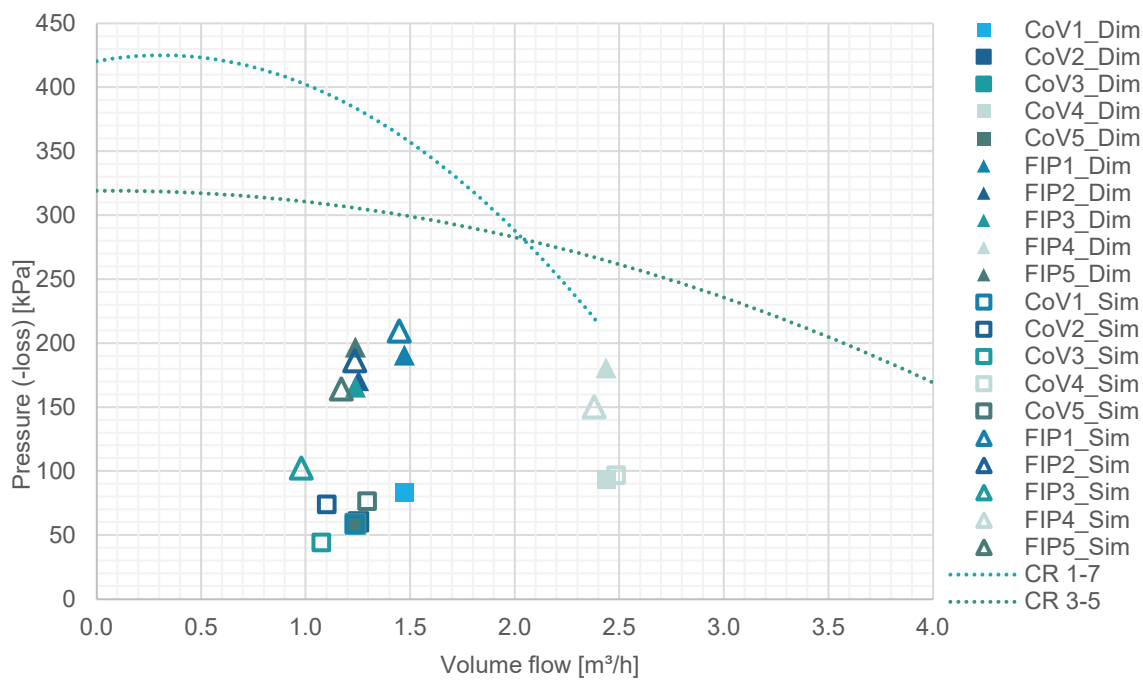


Figure 15: Pump curves at maximal pump speed and dimensioned and simulated operating points of FIPs and CoVs during design states

The operating point deviations of the actuators (FIP3, CoV3, FIP5, FIP4 and CoV1) can be explained by the positive ΔT_{set}^{prim} errors at the consuming Pros1 in Sc1 and Sc3 and the consuming Pros4 in Sc4. It is notable that FIP1, despite a positive ΔT_{set}^{prim} error during Sc1 has a higher head than expected. That is because in Sc1 the ΔT_{set}^{prim} error at the CoV4 in the DHC of FIP1 is negative due to the significant negative ΔT_{set}^{prim} error at the part-load FIP3. The difference between the simulation and design for CoV2 and CoV5 stems from a combination of ΔT_{set}^{prim} errors and the partially closed state of the CoVs $\kappa_{set}^{CoV2} = 0.8$ during Sc2 and $\kappa_{set}^{CoV5} = 0.93$ in Sc1 (see Table 17).

Due to the ΔT_{set}^{prim} errors, the predicted network states are not recreated fully in the simulation. However, overall, the deviations at the design load scenarios Sc1 and Sc2 are relatively small, and all actuators are well within their specified operating range.

Thus, the case study still yields relevant results for validating the dimensioning method under the third criterion. Furthermore, the positive outcomes in the second validation criterion showed that the divergent operating points did not impair the network's functionality. A pump-blocking effect, described in previous work on PBNs [47], could not be observed in the simulated exchange scenarios. It is possible that pump blocking is mitigated by the design method used for the FIPs, which considers the pressure conditions created by other prosumers at the feed-in location. However, this cannot be concluded definitively since pump blocking is more severe when prosumers of different sizes act together, and the prosumer powers in the case study PBN are relatively similar. [38]

With the validated PBN component sizes, and the CN components dimensioned in subsection 6.3.2, a comparative economic analysis between the PBN and CN variants is conducted in the next chapter.

8. Economic analysis

Since this thesis is focused on the primary network infrastructure, the secondary side characteristics are only considered if necessary. Thus, the economic comparisons in sections 8.1 and 8.2.1 just include secondary side components which are typical and essential for the two network types. Heat generators, storage, and expansion vessels are excluded from the investigation. For a simplified analysis of demand-related costs in 8.2.2, the yearly heat demand of prosumers is estimated with full-load hours, and the annual costs of example heat generators are included.

8.1. Investment costs and annuity

The investment costs are based on example offers or manufacturer price sheets, if available. Otherwise, prices are calculated from statistical values or cost catalogs. Figure 16 compares the investment costs of the case study networks. A more detailed list of the investment costs is provided in the appendix (see Table A.1 and Table A.2). An assumed flat rate increase of 20 % on the listed prices for accessories is included in the investment costs. The allocation of the data points is documented in Table A.4.

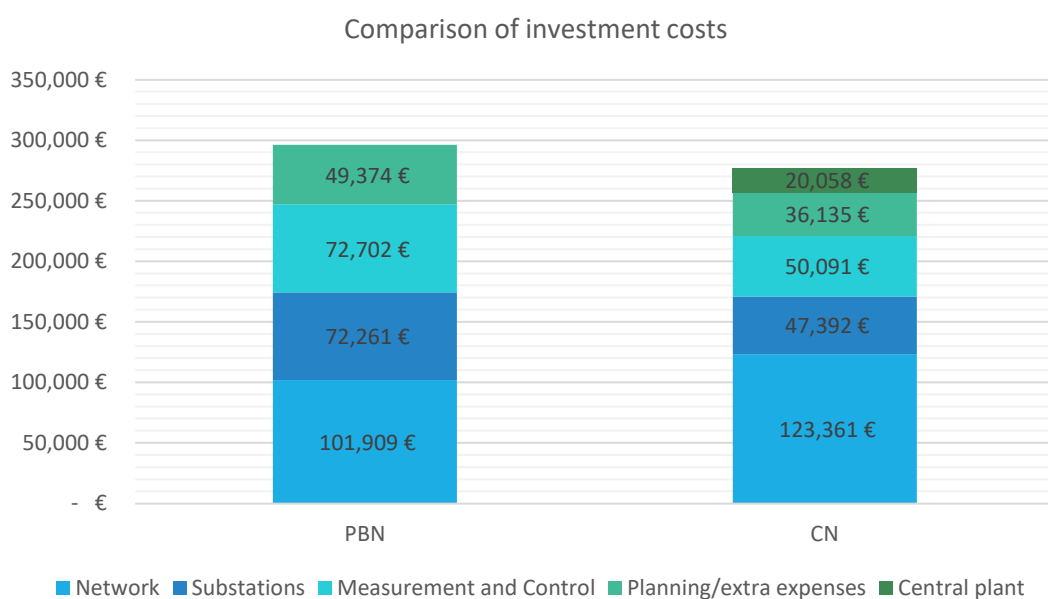


Figure 16: Comparison of the investment costs of the PBN and CN case study networks

In Figure 16, the higher costs for the elaborate substations (52 %) as well as measurement and control (45 %) for the PBN compared to the CN becomes apparent. This is mainly due

to the increased number of actuators needed for the flexible, bidirectional operation principle. The total cost difference between the variants is 19,207 €. It should be noted that investment costs of the building space needed for the substations and heat central(s) are not included in the comparison due to high uncertainties for the costs in this fictional consideration.

The annuity costs for capital and operational expenses of the two variants are compared based on the statistical values for life cycles and the percentual operational costs described in the VDI2067 (see Table A.3). The calculation of the annual capital-related costs is shown in equation (15).

$$A_{crc} = I * (1 + r)^L * \left(\frac{r}{(1 + r)^L - 1} \right) \quad (15)$$

Where A_{crc} is the annual capital-related cost in [€/a]

I is the investment cost in [€]

r is the interest rate in [%]

L is the life cycle in years [a]

The interest rate used in the base case is 3.5 %. The comparison of the annual capital-related costs is shown in Figure 17.

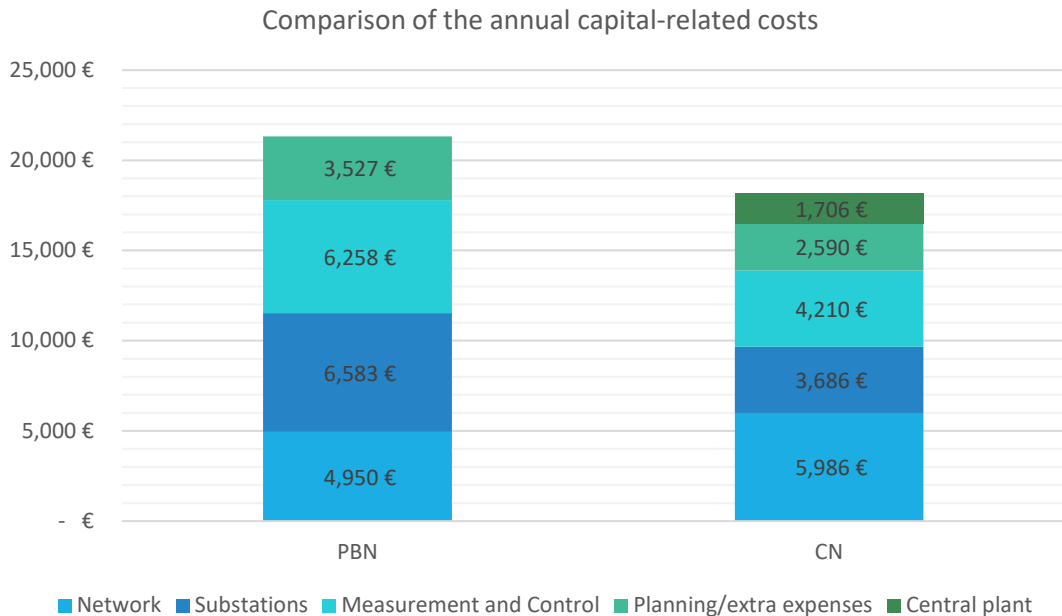


Figure 17: Comparison of the annual capital-related costs of the PBN and CN case study networks

The relative difference in substation costs (79 %) is even more significant in the annuity cost comparison due to the short life cycle of the installed active actuators of only ten years.

The total annual capital-related cost difference between the two variants is 3,401 €/a. A possibility to slightly reduce the investment costs in the PBN substation could be adjusting the secondary side layout to a bidirectional valve system so that only one pump and two three-way valves are needed to achieve bidirectional flows, as shown in [38].

The annual operation-related costs are calculated with the simple multiplication shown in equation (16).

$$A_{orc} = I * (f_{maint} + f_{s+insp}) \quad (16)$$

Where A_{orc} is the annual operation-related cost in [€/a]

I is the investment cost in [€]

f_{maint} is the effort for maintenance in [%/a]

f_{s+insp} is the effort for servicing and inspection in [%/a]

The values used for f_{maint} and f_{s+insp} are documented in the appendix (see Table A.3).

The comparison of the annual operation-related costs is shown in Figure 18.

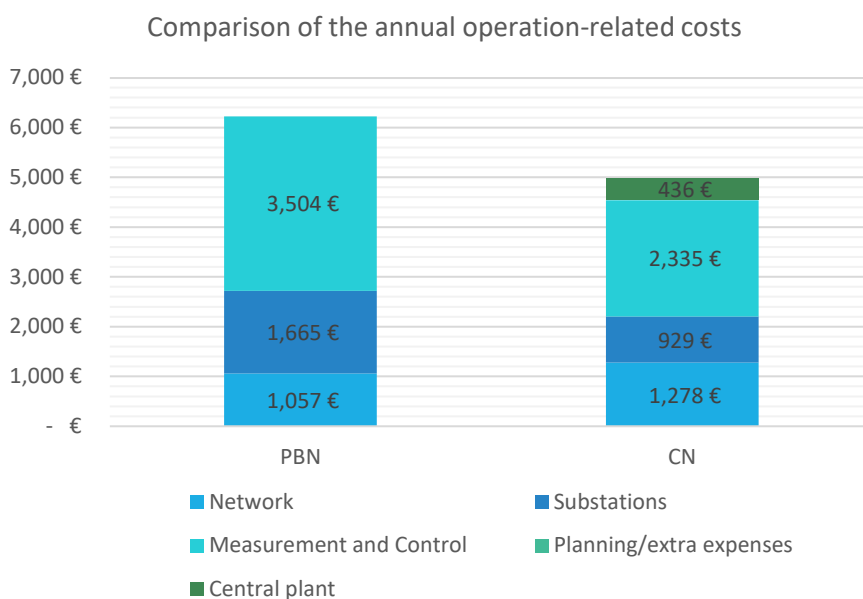


Figure 18: Comparison of the annual operation-related costs of the PBN and CN case study networks

The high share of measurement and control in operation-related costs for the PBN becomes apparent. The annual operation-related costs due to measurement and control in the PBN are 50 % higher than in the CN variant. The total annual operation-related cost difference between the variants is 1,248 €/a. Thus, the combined annual capital- and operation-related cost for the PBN is 4,390 €/a higher than in the CN variant.

8.2. Sensitivity analysis

Since the qualitative comparison of the economic sensitivity in subsection 4.2 concluded different behaviors for various influencing factors, a quantitative sensitivity analysis for the results of subsection 8.1 is conducted. Due to time constraints, only influencing factors that do not require a new dimensioning of the network components were considered. The four influence factors chosen for the sensitivity analysis were:

1. interest rate,
2. network length,
3. full-load hours,
4. energy cost.

8.2.1. Sensitivity of capital- and operation-related costs

The two influencing factors, interest rate and network length, are applied to the annual costs presented in Figure 17 and Figure 18. The results of the sensitivity analysis are shown in Figure 19.

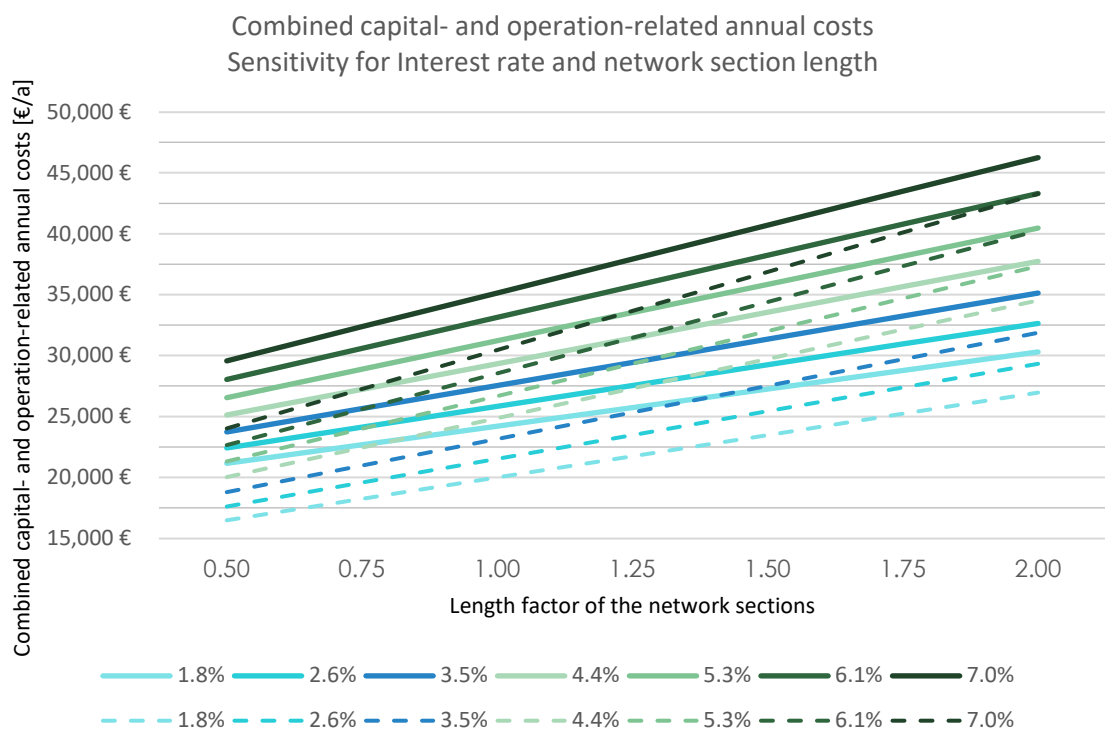


Figure 19: Sensitivity analysis for the annual costs of the PBN (solid lines) and CN (dashed lines) for changing interest rate and network section length

The higher sensitivity of the CN (dashed lines) towards changes in the network lengths is visible by the greater slope along the x-axis compared to the PBN (solid lines). For the base interest rate of 3.5 %, the total annual cost difference between the two variants is reduced by 26 % to 3,260 €/a at a network length factor of 2. This is due to the extra network section needed to connect the heating central and the larger pipe diameters needed in the CN variant (see subsection 6.3). This behavior confirms the qualitative deductions in subsection 4.2. However, the sensitivity towards a changing interest rate behaves differently than predicted in 4.2. The annual costs for the CN increased more strongly with a rising interest rate compared to the PBN. For the PBN, the mean increase in annual costs when raising the interest rate from 1.8 % to 7.0 % is 47 %. For the CN, the mean annual cost increase is 54 %. Two factors can explain this. First, the shorter lifespans of the components in PBNs reduce the impact of the interest rate-related costs in the annual capital-related costs (see equation (15)). Second, the share of annual operation-related costs for the PBN (23 %) is slightly larger than in the CN variant (21 %). Since a changing interest rate does not impact these costs, the impact on the total annual PBN costs is further reduced.

8.2.2. Sensitivity of demand-related costs

The annual capital- and operation-related costs for the PBN are higher than for the CN, and only a reduction in demand-related costs makes a break-even of the annual costs possible. The considered influencing factors for demand-related costs, full-load hours, and energy costs require assumptions on the generation technology in the network. Thus, the investment cost calculation is extended with heat generators. For the case study, gas boilers were chosen. For the CN, a required full redundancy is assumed, while no redundancy is needed in the PBN due to the flexible supply from other prosumers. The heat generators were dimensioned for the peak demand of the prosumers without a simultaneity factor. Vaillant gas condensing boilers were used as a manufacturing example [90]. The chosen heat generators for both network types are listed in Table 18.

Table 18: Chosen Vaillant [90] heat generators for the economic analysis of the case study PBN and CN

Description	Network	Investment costs			Capital-related costs		Op.-related costs	
		Units	Unit price	Total [€]	Lifecycle [a]	[€/a]	[%/a]	[€/a]
VC 25 CS/1-7 E/LL/P ecoTEC	PBN	4	5,882 €	23,530 €	18	1,784 €	3	706 €
ecoVIT exclusiv VKK 476/4 E	PBN	1	8,528 €	8,528 €	18	647 €	3	256 €
VKK1606/3-E ecoCRAFT	CN	2	18,266 €	36,533 €	20	2,570 €	2.5	913 €

With the annual capital- and operation-related costs of the heat generators listed in Table 18, the annual costs depicted in Figure 17 and Figure 18 can be updated. The resulting annual costs are shown in Figure 20.

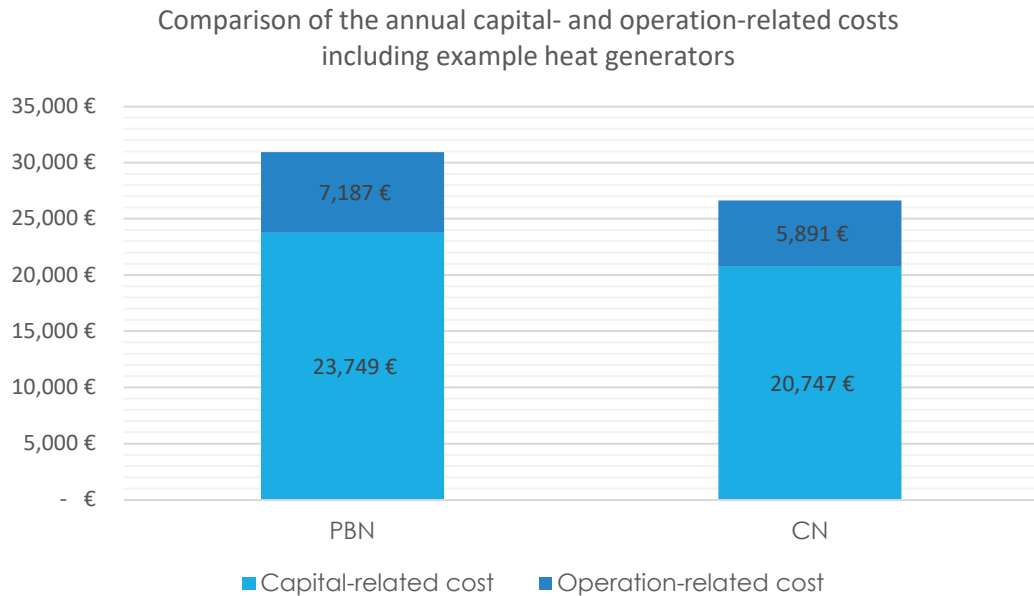


Figure 20: Comparison of the annual capital- and operation-related costs of the PBN and CN - including heat generators

With the heat generators included, the total annual capital- and operation-related cost difference between the variants is **4,298 €**.

Figure 21 shows the required reduction of demand-related costs needed for the PBN to break even with the annual costs of the CN. This could be achieved by increasing energy efficiency or reducing heat production costs. An efficiency increase could be achieved, for example, with reduced network losses or by reducing the operation time of generators in unfavorable states. A reduction of the heat production costs could be achieved by exploiting decentral, cost-efficient, renewable heat sources the CN structure would not allow.

In the base case scenario, 1300 full-load hours for the heat generators and a gas price of 12 ct/kWh are assumed. In this case, with the total peak heat demand of all prosumers (see Table 5) of 131.1 kW, a yearly demand of 170,426 kWh/a is estimated.

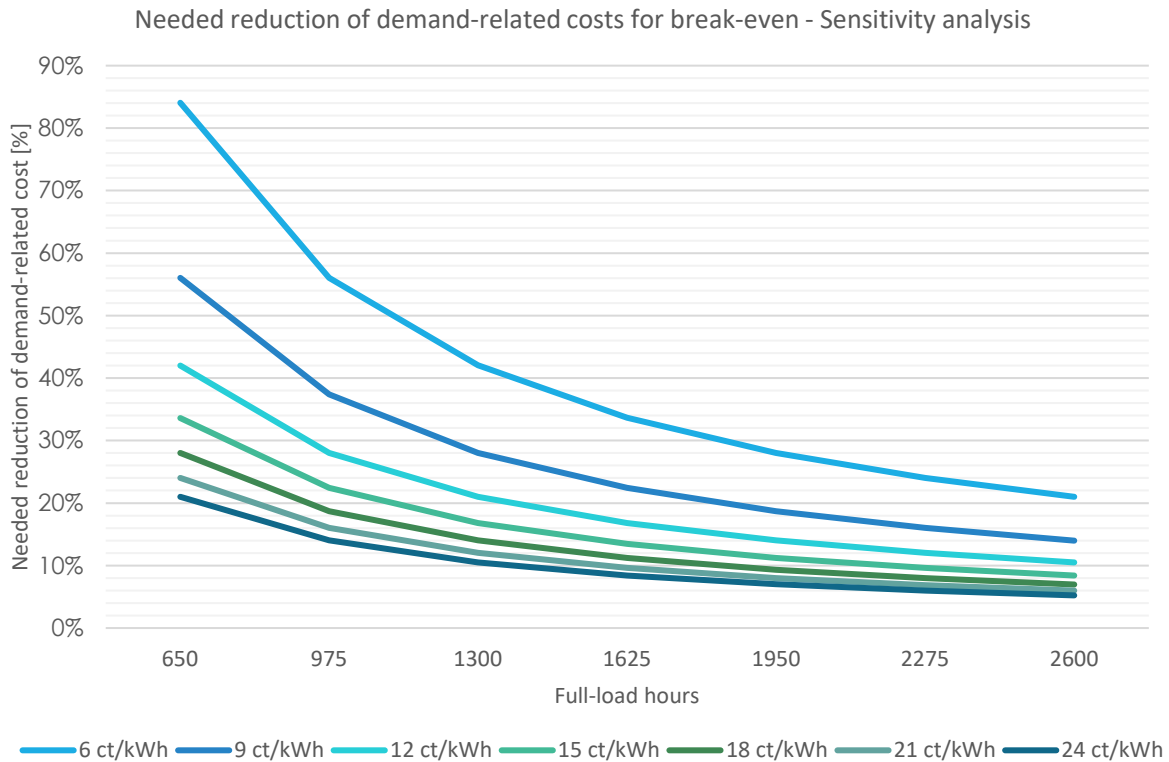


Figure 21: Needed reduction in demand-related costs in the PBN to break even with the annual CN costs - sensitivity analysis for full-load hours and energy cost

The required cost reduction shown in Figure 21 lies between 5 % and 84 %. For the base scenario, a reduction of demand-related costs by 21 % is needed to break even with the annual CN costs. Thus, either the heat demand is reduced by 35,789 kWh/a with the PBN variant, or the mixed heat production price is reduced to 9.48 ct/kWh. Naturally, combining the two factors to reduce the demand-related costs is viable to break even in annual costs. Bünning et al. observed reductions in energy costs by 53 % and 57 % with a bidirectional low-temperature network in comparison to CNs [14]. Although they investigated a combined heating and cooling supply, it still shows the potential for demand-related cost savings with optimized bidirectional prosumer networks. Kauko et al. described a possible reduction of heat demand by 25 % compared to a CN by implementing decentral prosumers and utilizing local low-temperature heat sources in a low-temperature network for a case study in Trondheim [15]. Thus, the needed reduction of 21 % in the base case comparison lies within an achievable range.

9. Conclusion and outlook

9.1. Conclusion

This thesis investigated the techno-economic differences between conventional thermal networks and thermal networks with prosumers. The literature review in Chapter 2 summarized the peculiarities of CN and PN network types and led to the research questions formulated in Chapter 3. They were focused on (i) analyzing the performance of CNs and PNs qualitatively, (ii) adapting conventional dimensioning methods to PBNs, and (iii) assessing the economic viability of PBNs. In Chapter 4, a qualitative comparison of the strengths, weaknesses, and economic sensitivities of the two network principles was performed based on a literature review. Chapter 5 described how conventional dimensioning methods were adapted to line PBNs. Additionally, the dimensioning tool, built to automate the proposed dimensioning process, was described. Subsequently, in Chapter 6, the network characteristics for the case study were defined, and the resulting component sizes for the PBN and the CN were summarized. Since a novel approach for dimensioning PBNs was used, the chosen component sizes were validated by analyzing the thermohydraulic states in a simulation, and by comparing them to the design states calculated with the dimensioning tool. After the PBN component sizes were validated, a comparative economic analysis for the PBN and the CN was conducted in Chapter 8.

The following findings resulted from the qualitative comparison of the two network operating principles:

1. PNs are generally more flexible than CNs.
2. PNs are generally more energy efficient than CNs.
3. PNs are generally more challenging to operate and control than CNs.
4. PNs generally cause higher capital- and operation-related costs than CNs.
5. The most relevant influencing factors for an economic sensitivity analysis between CNs and PNs are pipe diameter, interest rate, fuel price, full-load hours, availability of renewable energies, and network length.

The primary outcomes of the investigations on adapting conventional design methods to prosumer-based networks were:

1. The unclarity of the design conditions in PBNs due to changing hydraulic circuits requires a novel approach to determine the design states of network components.

2. An algorithm was proposed to calculate the design conditions of all network components in line PBNs based on the possible energy exchanges.
3. An Excel-based tool was built to automate the proposed dimensioning process.

The dimensioning of CN and PBN components for a case study with the same boundary conditions revealed that:

1. CNs require larger distribution pipes due to the layout of the network.
2. Pressure-independent control valves in CNs reduce the pump head drastically.

The investigation of three validation criteria for the designed PBN components by means of a thermohydraulic simulation led to these conclusions:

1. The algorithm to determine the power flows in the network pipe is accurate.
2. All prosumers are supplied sufficiently during design load and part-load situations.
3. The exact network conditions and actuator operating states could not be fully achieved with the used controller (especially in part-load situations). However, the deviations did not impair the functionality of the network, and in principle, the decentral actuators behaved as desired.
4. Overall, the dimensioned components are suited for a functional operation of the case study PBN.

The analysis of the economic performance of the two network types led to the following findings:

1. The high number of actuators in the elaborate PBN substations and the high effort for measurement and control cause greater annual capital- and operation-related costs compared to the CN. This is in agreement with the hypotheses in section 4.1.
2. The CN is more sensitive to a changing network length, as predicted in subsection 4.2.
3. The PBN is less sensitive than the CN to a changing interest rate, contrary to the prognosis in subsection 4.2. This is mainly due to the short life cycles of the increased number of actuators in the PBN.
4. Increasing energy costs and full-load hours facilitate the PBN to break even on the annual costs of a CN by reducing the demand-related costs with increased efficiency or reduced heat production costs. In the considered base case, a reduction of the demand-related costs by 21 % is required to break even.

In summary, the results of this thesis support that the presented static design approach is suitable for dimensioning small-scale line PBNs with limited information. Thus, the proposed method can be used in early-stage dimensioning and provides realistic component sizes for planners as a basis for variant comparisons and economic analyses. The viability of PBNs compared to CNs is highly sensitive to multiple influencing factors. However, higher capital- and operation-related costs are generally expected for PBNs, and thus, the economic viability is heavily dependent on the potential to increase efficiency or to implement cheap, renewable energies into the heat mix. There are many decentral heat sources in urban environments that can be efficiently utilized with heat pumps [15]. Additionally, costs for fossil energy carriers are expected to increase alongside rising carbon prices [91, 92]. Thus, the viability of PBNs can be assumed to increase as well.

9.2. Outlook

Additional research regarding PBN dimensioning should aim to advance the proposed dimensioning method towards more complex network typologies and conduct tests for different distributions of source and sink powers at the prosumers. Further investigations are needed to clarify the potential of an adapted substation design with pressure-independent control valves and a bidirectional valve system. For larger PBNs with more prosumers, simultaneity factors should be implemented in the dimensioning method. Combining the PBN structure with 5th generation district heating and cooling network principles could provide additional flexibility and efficient energy exchange benefits. The coupling with secondary load and production models for a dynamic simulation with included environmental influences on the prosumer side should be targeted for a more thorough investigation of the network's robustness. The potential for reducing demand-related costs needs to be investigated in more detail with an overarching energy management system. Overall, efforts for robust and consistent control strategies should be continued to facilitate the implementation of PBNs. With an increased standardization of the novel network type and progressively more favorable conditions, PBNs can be expected to become more relevant in future variant decisions.

References

- [1] Europäische Kommission, "Mitteilung der Kommission an das Europäische Parlament, den Rat, den europäischen Wirtschafts- und Sozialausschuss und den Ausschuss der Regionen: Der europäische Grüne Deal," Brüssel, 2019.
- [2] Energy, *Energy performance of buildings directive*. [Online]. Available: https://energy.ec.europa.eu/topics/energy-efficiency/energy-efficient-buildings/energy-performance-buildings-directive_en (accessed: Feb. 24 2023).
- [3] Publication Office/CORDIS, *Periodic Reporting for period 1 - RESHeat (RENEWABLE ENERGY SYSTEM FOR RESIDENTIAL BUILDING HEATING AND ELECTRICITY PRODUCTION) | H2020 | CORDIS | European Commission*. [Online]. Available: <https://cordis.europa.eu/project/id/956255/reporting> (accessed: Feb. 24 2023).
- [4] Energy, *Heating and cooling*. [Online]. Available: https://energy.ec.europa.eu/topics/energy-efficiency/heating-and-cooling_en (accessed: Feb. 24 2023).
- [5] H. Lund, B. Möller, B. V. Mathiesen, and A. Dyrelund, "The role of district heating in future renewable energy systems," *Energy*, vol. 35, no. 3, pp. 1381–1390, 2010, doi: 10.1016/j.energy.2009.11.023.
- [6] Urban Persson (urbper), "STRATEGO-WP2-Background-Report-4-Heat-Cold-Demands," [Online]. Available: <https://heatroadmap.eu/wp-content/uploads/2018/09/STRATEGO-WP2-Background-Report-4-Heat-Cold-Demands.pdf>
- [7] *World urbanization prospects: The 2018 revision*. New York: United Nations, 2019.
- [8] H. Kauko, K. H. Kvalsvik, D. Rohde, A. Hafner, and N. Nord, "Dynamic modelling of local low-temperature heating grids: A case study for Norway," *Energy*, vol. 139, pp. 289–297, 2017, doi: 10.1016/j.energy.2017.07.086. [Online]. Available: <https://www.sciencedirect.com/science/article/pii/S036054421731263X>
- [9] A. Revesz *et al.*, "Developing novel 5th generation district energy networks," *Energy*, vol. 201, p. 117389, 2020, doi: 10.1016/j.energy.2020.117389.
- [10] L. Brange, J. Englund, and P. Lauenburg, "Prosumers in district heating networks – A Swedish case study," *Applied Energy*, vol. 164, no. 1, pp. 492–500, 2016, doi: 10.1016/j.apenergy.2015.12.020.
- [11] H. Lund, P. A. Østergaard, D. Connolly, and B. V. Mathiesen, "Smart energy and smart energy systems," *Energy*, vol. 137, pp. 556–565, 2017, doi: 10.1016/j.energy.2017.05.123.
- [12] IEA, *Electrification – Analysis - IEA*. [Online]. Available: <https://www.iea.org/reports/electrification> (accessed: Mar. 12 2023).
- [13] S. Chicherin, A. Volkova, and E. Latõšov, "GIS-based optimisation for district heating network planning," *Energy Procedia*, vol. 149, pp. 635–641, 2018, doi: 10.1016/j.egypro.2018.08.228.
- [14] F. Bünning, M. Wetter, M. Fuchs, and D. Müller, "Bidirectional low temperature district energy systems with agent-based control: Performance comparison and operation optimization," *Applied Energy*, vol. 209, pp. 502–515, 2018, doi: 10.1016/j.apenergy.2017.10.072.
- [15] Hanne Kauko, Karoline Husevåg Kvalsvik, Daniel Rohde, Natasa Nord, and Åmund Utne, "Dynamic modeling of local district heating grids with prosumers: A case study for Norway," *Energy*, vol. 151, pp. 261–271, 2018, doi: 10.1016/j.energy.2018.03.033. [Online]. Available: <https://www.sciencedirect.com/science/article/pii/S0360544218304316>
- [16] H. Lund *et al.*, "4th Generation District Heating (4GDH)," *Energy*, vol. 68, pp. 1–11, 2014, doi: 10.1016/j.energy.2014.02.089.
- [17] Marco Wirtz, Thomas Schreiber, and Dirk Müller, "Survey of 53 5th Generation District Heating and Cooling (5GDHC) Networks in Germany," 2022.
- [18] S. Buffa, M. Cozzini, M. D'Antoni, M. Baratieri, and R. Fedrizzi, "5th generation district heating and cooling systems: A review of existing cases in Europe," *Renewable and Sustainable Energy Reviews*, vol. 104, no. 6, pp. 504–522, 2019, doi: 10.1016/j.rser.2018.12.059.
- [19] H. Lund *et al.*, "Perspectives on fourth and fifth generation district heating," *Energy*, vol. 227, p. 120520, 2021, doi: 10.1016/j.energy.2021.120520.

- [20] J. Lindhe, S. Javed, D. Johansson, and H. Bagge, "A review of the current status and development of 5GDHC and characterization of a novel shared energy system," *Science and Technology for the Built Environment*, vol. 28, no. 5, pp. 595–609, 2022, doi: 10.1080/23744731.2022.2057111.
- [21] isoplus Fernwärmetechnik Vertriebsgesellschaft mbH, *Planungshandbuch: Kapitel 1 - Allgemein*. [Online]. Available: <https://www.isoplus.de/download/planungshandbuch.html> (accessed: Jun. 8 2022).
- [22] Danfoss, "Application-Handbook_sep14," [Online]. Available: https://files.danfoss.com/download/Heating/Handbooks/Application-Handbook_sep14.pdf
- [23] T. Nussbaumer, S. Thalmann, A. Jenni, and J. Ködel, *Planungshandbuch Fernwärme*, 1st ed. Ittigen: EnergieSchweiz Bundesamt für Energie BFE, 2021.
- [24] AGFW, *Hauptbericht*. [Online]. Available: <https://www.agfw.de/startseite/leitfaeden-umsetzungshilfen> (accessed: Nov. 20 2022).
- [25] ASHRAE, *District Heating and Cooling Guides*. [Online]. Available: <https://www.ashrae.org/technical-resources/bookstore/district-heating-and-cooling-guides> (accessed: Nov. 20 2022).
- [26] DIN, *Produkte*. [Online]. Available: <https://www.din.de/de/meta/suche/62730!search?query=Fernw%C3%A4rme> (accessed: Nov. 20 2022).
- [27] AGFW-Regelwerk. [Online]. Available: <https://www.agfw-regelwerk.de/> (accessed: Nov. 20 2022).
- [28] B. Rismanchi, "District energy network (DEN), current global status and future development," *Renewable and Sustainable Energy Reviews*, vol. 75, pp. 571–579, 2017, doi: 10.1016/j.rser.2016.11.025.
- [29] S. Buffa, M. H. Fouladfar, G. Franchini, I. Lozano Gabarre, and M. Andrés Chicote, "Advanced Control and Fault Detection Strategies for District Heating and Cooling Systems—A Review," *Applied Sciences*, vol. 11, no. 1, p. 455, 2021, doi: 10.3390/app11010455.
- [30] AECOM and Energy Technologies Institute (ETI), "Tech. rep. Reducing the capital cost of district heat network infrastructure," 2017.
- [31] S. Chicherin, A. Zhuikov, and L. Junussova, "The new method for hydraulic calculations of a district heating (DH) network," *Energy*, p. 125071, 2022, doi: 10.1016/j.energy.2022.125071.
- [32] J. Maria Jebamalai, K. Marlein, J. Laverge, L. Vandeveld, and M. van den Broek, "An automated GIS-based planning and design tool for district heating: Scenarios for a Dutch city," *Energy*, vol. 183, pp. 487–496, 2019, doi: 10.1016/j.energy.2019.06.111.
- [33] Y. Merlet, R. Baviere, and N. Vasset, "Formulation and assessment of multi-objective optimal sizing of district heating network," *Energy*, vol. 252, p. 123997, 2022, doi: 10.1016/j.energy.2022.123997.
- [34] J. Röder, B. Meyer, U. Krien, J. Zimmermann, T. Stührmann, and E. Zondervan, "Optimal Design of District Heating Networks with Distributed Thermal Energy Storages – Method and Case Study," 2021, doi: 10.5278/IJSEPM.6248.
- [35] H. Wang, H. Wang, H. Zhou, and T. Zhu, "Modeling and optimization for hydraulic performance design in multi-source district heating with fluctuating renewables," *Energy Conversion and Management*, vol. 156, pp. 113–129, 2018, doi: 10.1016/j.enconman.2017.10.078.
- [36] N. Wang *et al.*, "Hydraulic resistance identification and optimal pressure control of district heating network," *Energy and Buildings*, vol. 170, pp. 83–94, 2018, doi: 10.1016/j.enbuild.2018.04.003.
- [37] R. Bavière and M. Vallée, "Optimal Temperature Control of Large Scale District Heating Networks," *Energy Procedia*, vol. 149, pp. 69–78, 2018, doi: 10.1016/j.egypro.2018.08.170.
- [38] T. Sommer, M. Sulzer, M. Wetter, A. Sotnikov, S. Mennel, and C. Stettler, "The reservoir network: A new network topology for district heating and cooling," *Energy*, vol. 199, p. 117418, 2020, doi: 10.1016/j.energy.2020.117418.
- [39] M. A. Ancona, L. Branchini, A. de Pascale, and F. Melino, "Smart District Heating: Distributed Generation Systems' Effects on the Network," *Energy Procedia*, vol. 75, pp. 1208–1213, 2015, doi: 10.1016/j.egypro.2015.07.157.

- [40] M. Pipiciello, M. Caldera, M. Cozzini, M. A. Ancona, F. Melino, and B. Di Pietra, “Experimental characterization of a prototype of bidirectional substation for district heating with thermal prosumers,” *Energy*, vol. 223, p. 120036, 2021, doi: 10.1016/j.energy.2021.120036.
- [41] T. Lickleder, T. Hamacher, M. Kramer, and V. S. Perić, “Thermohydraulic model of Smart Thermal Grids with bidirectional power flow between prosumers,” *Energy*, vol. 230, 2021, doi: 10.1016/j.energy.2021.120825. [Online]. Available: <https://www.sciencedirect.com/science/article/pii/S0360544221010732>
- [42] D.-I. Stanica, M. Bachmann, and M. Kriegel, “Design and performance of a multi-level cascading district heating network with multiple prosumers and energy storage,” *Energy Reports*, vol. 7, pp. 128–139, 2021. [Online]. Available: <https://www.sciencedirect.com/science/article/pii/S2352484721007666>
- [43] S. R. Jones *et al.*, “A System Design for Distributed Energy Generation in Low-Temperature District Heating (LTDH) Networks,” *Future Cities and Environment*, vol. 5, no. 1, 2019, doi: 10.5334/fce.44.
- [44] L. Brand, A. Calvén, J. Englund, H. Landersjö, and P. Lauenburg, “Smart district heating networks – A simulation study of prosumers’ impact on technical parameters in distribution networks,” *Applied Energy*, vol. 129, no. 4, pp. 39–48, 2014, doi: 10.1016/j.apenergy.2014.04.079.
- [45] Lisa Brange, “Technical and Environmental Analysis of Prosumers in District Heating Networks,” Licentiate in Engineering, Division of Efficient Energy Systems, Lund University, 2015.
- [46] I. B. Hassine and U. Eicker, “Control Aspects of Decentralized Solar Thermal Integration into District Heating Networks,” *Energy Procedia*, vol. 48, pp. 1055–1064, 2014. [Online]. Available: <https://www.sciencedirect.com/science/article/pii/S1876610214003828>
- [47] T. Lickleder, D. Zinsmeister, I. Elizarov, V. Perić, and P. Tzscheuschler, “Characteristics and Challenges in Prosumer-Dominated Thermal Networks,” *J. Phys.: Conf. Ser.*, vol. 2042, no. 1, 2021, doi: 10.1088/1742-6596/2042/1/012039. [Online]. Available: <https://iopscience.iop.org/article/10.1088/1742-6596/2042/1/012039>
- [48] M. Wetter and J. Hu, *Quayside energy system analysis*, 2019.
- [49] T. Sommer *et al.*, “Hydrothermal challenges in low-temperature networks with distributed heat pumps,” *Energy*, p. 124527, 2022, doi: 10.1016/j.energy.2022.124527.
- [50] Ilya Elizarov, *Analysis, Modelling, and Control Strategy Development for Prosumer-based Heat Networks*, 2020. [Online]. Available: https://www.researchgate.net/publication/343136226_Analysis_Modelling_and_Control_Strategy_Development_for_Prosumer-based_Heat_Networks
- [51] I. Elizarov and T. Lickleder, “ProsNet – a Modelica library for prosumer-based heat networks: description and validation,” *Journal of Physics: Conference Series (JPCS)*, vol. 2042, no. 1, p. 12031, 2021, doi: 10.1088/1742-6596/2042/1/012031. [Online]. Available: <https://github.com/thomaslickleder/ProsNet>
- [52] G. Schweiger, P.-O. Larsson, F. Magnusson, P. Lauenburg, and S. Velut, “District heating and cooling systems – Framework for Modelica-based simulation and dynamic optimization,” *Energy*, vol. 137, no. 3, pp. 566–578, 2017, doi: 10.1016/j.energy.2017.05.115.
- [53] M. Bilardo, F. Sandrone, G. Zanzottera, and E. Fabrizio, “Modelling a fifth-generation bidirectional low temperature district heating and cooling (5GDHC) network for nearly Zero Energy District (nZED),” *Energy Reports*, vol. 7, pp. 8390–8405, 2021, doi: 10.1016/j.egyr.2021.04.054.
- [54] T. Lickleder, D. Zinsmeister, and V. S. Perić, “A field-level control approach for bidirectional heat transfer stations in prosumerbased thermal networks: simulation and experimental evaluation: Presentation at “8th International Conference on Smart Energy Systems.”,” pp. 62–63. [Online]. Available: https://smartenergysystems.eu/wp-content/uploads/2022/09/BoA_SESAU2022.pdf
- [55] J. Zeng, J. Han, and G. Zhang, “Diameter optimization of district heating and cooling piping network based on hourly load,” *Applied Thermal Engineering*, vol. 107, pp. 750–757, 2016, doi: 10.1016/j.applthermaleng.2016.07.037. [Online]. Available: <https://www.sciencedirect.com/science/article/pii/S1359431116311668>

- [56] H. Ren, Q. Wu, Q. Li, and Y. Yang, "Optimal design and management of distributed energy network considering both efficiency and fairness," *Energy*, vol. 213, p. 118813, 2020, doi: 10.1016/j.energy.2020.118813.
- [57] B. Manrique Delgado *et al.*, "Lifecycle cost and CO2 emissions of residential heat and electricity prosumers in Finland and the Netherlands," *Energy Conversion and Management*, vol. 160, pp. 495–508, 2018, doi: 10.1016/j.enconman.2018.01.069. [Online]. Available: <https://www.sciencedirect.com/science/article/pii/S0196890418300827>
- [58] S. Buffa, A. Soppelsa, M. Pipiciello, G. Henze, and R. Fedrizzi, "Fifth-Generation District Heating and Cooling Substations: Demand Response with Artificial Neural Network-Based Model Predictive Control," *Energies*, vol. 13, no. 17, p. 4339, 2020, doi: 10.3390/en13174339.
- [59] M. Sulzer, N. Vetterli, E. Thaler, and P. Ryser, *Monitoring Suurstoffi, Auswertung Okt. 2013 – Sep. 2016*, 2017.
- [60] A. Revesz *et al.*, "A holistic design approach for 5th generation smart local energy systems: Project GreenSCIES," *Energy*, vol. 242, p. 122885, 2022, doi: 10.1016/j.energy.2021.122885.
- [61] D. Zinsmeister *et al.*, "A Prosumer-Based Sector-Coupled District Heating and Cooling Laboratory Architecture," *SSRN Journal*, 2022, doi: 10.2139/ssrn.4003819.
- [62] F. Speer, T. Lickleder, D. Zinsmeister, and V. Perić, "Dimensioning radial prosumer-based thermal networks," *IEWT*, 2023. [Online]. Available: https://iewt2023.eeg.tuwien.ac.at/download/contribution/fullpaper/104/104_fullpaper_20230210_224423.pdf
- [63] K. Lichtenegger *et al.*, "Decentralized heating grid operation: A comparison of centralized and agent-based optimization," *Sustainable Energy, Grids and Networks*, vol. 21, p. 100300, 2020, doi: 10.1016/j.segan.2020.100300.
- [64] M. Gross, B. Karbasi, T. Reiners, L. Altieri, H.-J. Wagner, and V. Bertsch, "Implementing prosumers into heating networks," *Energy*, vol. 230, p. 120844, 2021, doi: 10.1016/j.energy.2021.120844.
- [65] H. Wang, H. Wang, and T. Zhu, "A new hydraulic regulation method on district heating system with distributed variable-speed pumps," *Energy Conversion and Management*, vol. 147, pp. 174–189, 2017, doi: 10.1016/j.enconman.2017.03.059.
- [66] Ilya Elizarov, *Analysis, Modelling, and Control Strategy Development for Prosumer-based Heat Networks*, 2020. [Online]. Available: https://www.researchgate.net/publication/343136226_Analysis_Modelling_and_Control_Strategy_Development_for_Prosumer-based_Heat_Networks
- [67] X. Sheng and L. Duanmu, "Electricity consumption and economic analyses of district heating system with distributed variable speed pumps," *Energy and Buildings*, vol. 118, pp. 291–300, 2016, doi: 10.1016/j.enbuild.2016.03.005.
- [68] P. A. Østergaard *et al.*, "The four generations of district cooling - A categorization of the development in district cooling from origin to future prospect," *Energy*, vol. 253, p. 124098, 2022, doi: 10.1016/j.energy.2022.124098. [Online]. Available: <https://www.sciencedirect.com/science/article/pii/S0360544222010015>
- [69] T. Nussbaumer and S. Thalmann, "Dimensionierung von Fernwärmenetzen," *ingenieur.de*, 01 Feb., 2017. <https://www.ingenieur.de/fachmedien/bwk/energieversorgung/dimensionierung-von-fernwaermenetzen/> (accessed: Jul. 20 2022).
- [70] T. Nussbaumer and S. Thalmann, "Influence of system design on heat distribution costs in district heating," *Energy*, vol. 101, pp. 496–505, 2016, doi: 10.1016/j.energy.2016.02.062.
- [71] *ISOPlus-Website*. [Online]. Available: <https://www.isoplus.de/home.html> (accessed: Jan. 26 2023).
- [72] *PE Rohre für den Versorgungsbereich*. [Online]. Available: https://www.frank-gmbh.de/de/produkte/versorgung/rohre_pe_versorgung.php (accessed: Mar. 7 2023).
- [73] *Recknagel - Taschenbuch für Heizung + Klimatechnik 78. Ausgabe 2017/2018*. [s.l.]: Deutscher Industrieverlag, 2016.
- [74] D. J. Zigrang and N. D. Sylvester, "Explicit approximations to the solution of Colebrook's friction factor equation," *AIChE J.*, vol. 28, no. 3, pp. 514–515, 1982, doi: 10.1002/aic.690280323.

- [75] isoplus Fernwärmetechnik Vertriebsgesellschaft mbH, *Planungshandbuch: Kapitel 2 - STARRE VERBUNDSYSTEME*. [Online]. Available: <https://www.isoplus.de/download/planungshandbuch.html> (accessed: Jun. 8 2022).
- [76] *Thermal Network - CoSES Laboratory Documentation - TUM Wiki*. [Online]. Available: <https://wiki.tum.de/display/coseslab/Thermal+Network> (accessed: Mar. 12 2023).
- [77] *TABULA WebTool*. [Online]. Available: <https://webtool.building-typology.eu/#bm> (accessed: Jan. 24 2023).
- [78] M.-H. Kim, D.-W. Kim, D.-W. Lee, and J. Heo, "Experimental Analysis of Bi-Directional Heat Trading Operation Integrated with Heat Prosumers in Thermal Networks," *Energies*, vol. 14, no. 18, p. 5881, 2021, doi: 10.3390/en14185881.
- [79] *SWEP brazed plate heat exchangers - SWEP*. [Online]. Available: <https://www.swep.net/> (accessed: Mar. 8 2023).
- [80] *SWEP DThermX*. [Online]. Available: <https://dthermx.swep.net/login> (accessed: Mar. 10 2023).
- [81] Grundfos Product Center, *Produktauslegung*. [Online]. Available: <https://product-selection.grundfos.com/de/size-page?qcid=2050085854> (accessed: Mar. 10 2023).
- [82] Fr. Sauter AG, *2-Way Valve with Male Thread, PN16 - VUN On Fr. Sauter AG*. [Online]. Available: <http://bim.sauter-controls.com/viewitems/regulating-valves/2-way-valve-with-male-thread--pn16---vun> (accessed: Jan. 26 2023).
- [83] Grundfos Germany, *CR > Vertikale mehrstufige Kreiselpumpen / GG/1.4301*. [Online]. Available: <https://product-selection.grundfos.com/de/products/cr?tab=products> (accessed: Jan. 26 2023).
- [84] T. Nussbaumer, S. Thalman, A. Jenni, and S. Mennel, "Leitfaden zur Planung von Fernwärme-Übergabestationen," EnergieSchweiz, Bundesamt für Energie BFE, Ittigen, 2021.
- [85] SWM, "TAB-Heizwasser-Anlage 5.1-Kompaktstation kleiner 300 kW (Prinzipschema)," [Online]. Available: <https://www.swm.de/dam/doc/installateure/tab-heizwasser/tab-heizwasser-anlage-5-1-kompaktstation-kleiner-300-kw-prinzipschema.pdf>
- [86] Belimo, *Website*. [Online]. Available: https://www.belimo.com/de/de_CH/ (accessed: Mar. 8 2023).
- [87] Belimo, "Elektronisch druckunabhängiger Regelkugelhahn mit Energiemonitoring Belimo Energy Valve™," [Online]. Available: https://www.belimo.com/mam/europe/technical-documentation/project_planning_notes/belimo_notes-for-project-planning_EV4_de-ch.pdf
- [88] Belimo, "Technical data sheet EV.R2+BAC," [Online]. Available: https://www.belimo.com/mam/general-documents/datasheets/en-gb/belimo_EV.R2_BAC_datasheet_en-gb.pdf
- [89] *Dymola – Dassault Systèmes®*. [Online]. Available: <https://www.3ds.com/de/produkte-und-services/catia/produkte/dymola/> (accessed: Jan. 24 2023).
- [90] *Gasthermen und Gasheizungen finden | Vaillant*. [Online]. Available: https://www.vaillant.at/privatanwender/produkte/produktgruppe/gasheizungen/?facets=f%2Fmeta_main_energy_source%2Fgas (accessed: Mar. 13 2023).
- [91] "Europe carbon prices expected to rise to 2030-industry survey," *Reuters Media*, 14 Jun., 2021. <https://www.reuters.com/business/sustainable-business/europe-carbon-prices-expected-rise-2030-industry-survey-2021-06-14/#:~:text=The%20survey%20by%20the%20International%20Emissions%20Trading%20Association,free%20to%20Reuters%20and%20know%20the%20full%20story> (accessed: Mar. 13 2023).
- [92] Energy Post, *Calculating the effect of \$50/tonne CO2 on energy prices - Energy Post*. [Online]. Available: <https://energypost.eu/calculating-the-effect-of-50-tonne-co2-on-energy-prices/> (accessed: Mar. 13 2023).

Appendix

A. Economic analysis

Table A.1: Investment costs of the case study PBN

Pos.	Description	Amount	Unit	Price per unit	Investment cost
1	Network				101,909 €
1.1	Pavement	113	m ²	250 €	28,250 €
1.2	Excavation	101.7	m ³	100 €	10,170 €
1.3	Restoration	101.7	m ³	120 €	12,204 €
1.4	Disposal	79.1	m ³	72 €	5,695 €
1.5	Piping				
1.5.1	DN25	253	m	37 €	9,315 €
1.5.2	DN32	100	m	40 €	3,962 €
1.5.3	DN40	99	m	41 €	4,090 €
1.6	Fittings	1	Flat rate	13,026 €	13,026 €
1.7	Installation	1	Flat rate	15,197 €	15,197 €
2	Substations				72,261 €
2.1	Heat Exchangers				
2.1.1	B15Tx40	4	pcs	919 €	3,675 €
2.1.2	B15Tx50	1	pcs	1,065 €	1,065 €
2.2	Pumps primary				
2.2.1	CR 1-7 A-A-A-E-HQQE	4	pcs	3,039 €	12,156 €
2.2.2	CR 3-5 A-A-A-E-HQQE	1	pcs	3,218 €	3,218 €
2.3	Pumps secondary				
2.3.1	Generic Pump	10	pcs	1,500 €	15,000 €
2.4	Control valves				
2.4.1	VUN015F320	4	pcs	510 €	2,041 €
2.4.2	VUN015F310	1	pcs	507 €	507 €
2.4.3	VUN025F300	8	pcs	550 €	4,397 €
2.4.4	VUN032F300	2	pcs	611 €	1,222 €
2.5	Shut-off valves				
2.5.1	BOA-C, PN6 DN 25	16	pcs	278 €	4,447 €
2.5.2	BOA-C, PN6 DN 32	4	pcs	309 €	1,238 €
2.6	Check valves				
2.6.1	BOA-R, PN16 DN 25	12	pcs	181 €	2,169 €
2.6.2	BOA-R, PN16 DN 32	3	pcs	208 €	625 €
2.7	Fittings	5	Flat rate	500 €	2,500 €
2.8	Installation	5	Flat rate	3,600 €	18,000 €
3	Measurement and Control				72,702 €
3.1	Pressure gauges	20	pcs	50 €	1,000 €

3.2	Heat-meters/Flowmeters				
3.2.1	MultiCal 303 Qp 1,5	8	pcs	175 €	1,400 €
3.2.2	MultiCal 303 Qp 2,5	2	pcs	223 €	446 €
3.3	Thermometers	20	pcs	50 €	1,000 €
3.4	Fiber Optics	226	m	6 €	1,356 €
3.5	Data Points	135	pcs	400 €	67,500 €
Summary					246,871 €
4	Planning/extra expenses				49,374 €
Total					296,246 €

Table A.2: Investment costs of the case study CN

Pos.	Description	Amount	Unit	Price per unit	Total cost
1	Network				123,361 €
1.1	Pavement	133	m ²	250 €	33,250 €
1.2	Excavation	119.7	m ³	100 €	11,970 €
1.3	Restoration	119.7	m ³	120 €	14,364 €
1.4	Disposal	93.1	m ³	72 €	6,703 €
1.5	Piping				
1.5.1	DN25	173	m	37 €	6,370 €
1.5.2	DN32	20	m	40 €	792 €
1.5.3	DN40	179	m	41 €	7,396 €
1.5.4	DN50	160	m	45 €	7,185 €
1.6	Fittings	1	Flat rate	16,307 €	16,307 €
1.7	Installation	1	Flat rate	19,025 €	19,025 €
2	Central plant				20,058 €
2.1	Circulation pumps				
2.1.1	CR 10-3 A-A-A-E-HQQE	2	pcs	4,718 €	9,437 €
2.2	Check valves				
2.2.1	BOA-R, PN16 DN 50	2	pcs	403 €	806 €
2.3	Shut-off valves				
2.3.1	BOA-C, PN6 DN 50	4	pcs	392 €	1,566 €
2.4	Fittings	1	Flat rate	750 €	750 €
2.5	Installation	1	Flat rate	7,500 €	7,500 €
3	Substations				47,392 €
2.1	Heat Exchangers				
2.1.1	B15Tx40	4	pcs	919 €	3,675 €
2.1.2	B15Tx50	1	pcs	1,065 €	1,065 €
2.3	Pumps secondary				
2.3.1	Generic Pump	5	pcs	1,500 €	7,500 €
2.4	Energy valves				
2.4.1	EV020R2+BAC	4	pcs	1,598 €	6,394 €
2.4.2	EV025R2+BAC	1	pcs	1,642 €	1,642 €

2.5	Shut-off valves					
2.5.1	BOA-C, PN6 DN 25	16	pcs	278 €	4,447 €	
2.5.2	BOA-C, PN6 DN 32	4	pcs	309 €	1,238 €	
2.6	Check valves					
2.6.1	BOA-R, PN16 DN 25	4	pcs	181 €	723 €	
2.6.2	BOA-R, PN16 DN 32	1	pcs	208 €	208 €	
2.7	Fittings	5	Flat rate	500 €	2,500 €	
2.8	Installation	5	Flat rate	3,600 €	18,000 €	
4	Measurement and Control				50,091 €	
3.1	Pressure gauges	22	pcs	50 €	1,100 €	
3.2	Heat-meters/Flowmeters					
3.2.1	MultiCal 303 Qp 1,5	4	pcs	175 €	700 €	
3.2.2	MultiCal 303 Qp 2,5	1	pcs	223 €	223 €	
3.2.3	MultiCal 303 Qp 10	1	pcs	872 €	872 €	
3.3	Thermometers	22	pcs	50 €	1,100 €	
3.4	Fiber Optics	266	m	6 €	1,596 €	
3.5	Data Points	89	pcs	500 €	44,500 €	
	Summary				240,903 €	
5	Planning/extra expenses				36,135 €	
	Total				277,038 €	

Table A.3: Used life cycles and yearly operational costs, based on the VDI2067

Description	capital-related cost	operation-related cost
	Lifecycle [a]	$f_{maint} + f_{s+insp}$ [%/a]
Piping Network	40	1
Fittings Network	40	1
Pavement	40	1
Excavation	40	1
Restoration Excavation	40	1
Disposal Excavation	40	1
Installation Network	40	1
Heat exchanger	20	2
Circulation pump	10	3
Control valves	10	2.5
Check valves	20	2.5
Misc. Fittings	20	2.5
Shut-off valves	20	2.5
Fiber optics cables	40	1
Data points/Measurement and Control	15	5
Pressure gauge	15	3
Thermometer	15	3
Heat meter/Flow meter	15	3
Planning/extra expenses	20	0

Table A.4: Data points considered in the economic analysis;
AI: analog input, AO: analog output, DI: digital input, DO: digital output

Description	# pri side	# sec side	AI	AO	DI	DO	Sum
PBN-Substation							
Thermal sensor	2	3	1	0	0	0	5
Pressure-sensor	2	0	1	0	0	0	2
Heat meter	1	1	0	1	0	0	2
Pump	1	2	1	1	1	1	12
2W Valve	1	2	1	1	0	0	6
Subtotal	7	8					27
CN-Substation							
Thermal sensor	2	3	1	0	0	0	5
Pressure-sensor	2	0	1	0	0	0	2
Heat meter	1	0	0	1	0	1	2
Pump	0	1	1	1	1	1	4
2W Valve	1	0	1	1	0	0	2
Subtotal	6	4					15
CN-Heat central							
Thermal sensor	2	0	1	0	0	0	2
Pressure-sensor	2	0	1	0	0	0	2
Heat meter	1	0	0	1	0	1	2
Pump	2	0	1	1	1	1	8
2W Valve	0	0	1	1	0	0	0
Subtotal	7	0					14

B. Dimensioning tool

Table B.1: Pseudo-code nomenclature

Name	Description
Pipe_con_left	Maximal consumption power in a pipe from prosumers to the left
Pipe_pro_left	Maximal production power in a pipe from prosumers to the left
Pipe_con_right	Maximal consumption power in a pipe from prosumers to the right
Pipe_pro_right	Maximal production power in a pipe from prosumers to the right
Ppro	Production power of a prosumer
Pcon	Consumption power prosumer
Ppro_pipe	Maximal assigned prosumer production power to a pipe
Pcon_pipe	Maximal assigned prosumer consumption power to a pipe
Ppro_pros	Maximal production power of a prosumer
Pcon_pros	Maximal consumption power of a prosumer
ConnectionPipe	Pipe connecting prosumers to the main distribution line
LeftConnectionPipe	ConnectionPipe left of the considered DistributionPipe
RightConnectionPipe	ConnectionPipe right of the considered DistributionPipe
DistributionPipe	Pipe between two connection pipes, building the main distribution line
DistributionPipeLeft	DistributionPipe left of the considered ConnectionPipe
DistributionPipeRight	DistributionPipe right of the considered ConnectionPipe
LeftProsumers	Prosumers left of the considered DistributionPipe
RightProsumers	Prosumers right of the considered DistributionPipe
EnergyExchangeOne	Max. combination of Ppro from one prosumer and Pcon of another prosumer
EnergyExchangeTwo	Max. combination of Pcon from one prosumer and Ppro of another prosumer
Pros_pipe	ConnectionPipe assigned to a certain prosumer
Q_max_pro	Maximal possible production related power flow in the pipe
Q_max_con	Maximal possible consumption related power flow in the pipe
Q_max	Design power flow in a pipe
V_dot_con	Consumption power related volume flow
V_dot_pro	Production power related volume flow
First_pros_pro	First (leftmost) prosumer in production mode
Last_pros_pro	Last (rightmost) prosumer in production mode
First_pros_con	First (leftmost) prosumer in consumption mode
Last_pros_con	Last (rightmost) prosumer in consumption mode
dP_left	Pressure loss from a certain prosumer to a prosumer on the left
dP_right	Pressure loss from a certain prosumer to a prosumer on the right
dP_pipe	Pressure loss in a pipe during design power flow
dP_pros_pipes	Pressure loss in the network pipes for a certain prosumer connection
dP_pros	Relevant (max) pipe pressure loss for a certain prosumer
dP_valve_theo	Theoretically calculated pressure drop in the control valve
dP_valve_real	Real pressure drop in the control valve after dimensioning
dP_pros_pro_total	Total pressure drop relevant for the feed-in-pump of a certain prosumer

Maximum Power flow in pipes

ONE - Power flows in pipes

For First_pipe to Last_pipe 'calculate available power demand and supply in both directions

Pipe_con_left

IF Pipe is DistributionPipe THEN

 Pipe_con_left = Pcon_LeftConnectionPipe

ELSE

 Assign Pipe to Prosumer

 Pipe_con_left = Pcon_Pro

END IF

Pipe_pro_left

IF Pipe is DistributionPipe THEN

 Pipe_pro_left = Ppro_LeftConnectionPipe

ELSE

 Assign Pipe to Prosumer

 Pipe_pro_left = Ppro_Pro

END IF

Pipe_con_right

IF Pipe is DistributionPipe THEN

 Pipe_con_right = Pcon_RightConnectionPipe

ELSE

 Assign Pipe to Prosumer

 Pipe_con_right = Pcon_Pro

END IF

Pipe_pro_right

IF Pipe is DistributionPipe THEN

 Pipe_pro_right = Ppro_RightConnectionPipe

ELSE

 Assign Pipe to Prosumer

 Pipe_pro_right = Ppro_Pro

END IF

NEXT pipe

ANE - Power flows in pipes

For First_pipe to Last_pipe 'calculate available power demand and supply in both directions

Pipe_con_left

 IF Pipe is DistributionPipe THEN

 Pipe_con_left = \sum Pin_LeftProsumers

ELSE

 Assign Pipe to Prosumer

 Pipe_con_left = Pcon_Pro

END IF

Pipe_con_right

IF Pipe is DistributionPipe THEN

 Pipe_con_right = \sum Pcon_RightProsumers

ELSE

 Assign Pipe to Prosumer

 Pipe_con_right = Pcon_Pro

END IF

Pipe_pro_left

IF Pipe is DistributionPipe THEN

 Pipe_pro_left = \sum Ppro_LeftProsumers

ELSE

 Assign Pipe to Prosumer

 Pipe_pro_left = Ppro_Prosumer

END IF

XX

```

Pipe_pro_right
IF Pipe is DistributionPipe THEN
    Pipe_pro_right =  $\sum$ Ppro_RightProsumers

ELSE
    Assign Pipe to Prosumer
    Pipe_pro_right = Ppro_Pro

END IF

NEXT pipe

```

ANE and ONE max Power flow

```

FOR First_pipe to Last_pipe
    Q_max
    IF Pipe is DistributionPipe THEN
        MIN(Pipe_con_left; Pipe_pro_right) = EnergyExchangeOne
        MIN(Pipe_pro_left; Pipe_con_right) = EnergyExchangeTwo
        MAX(EnergyExchangeOne; EnergyExchangeTwo) = Q_max 'compare possible energy exchanges for max power flow

    ELSE
        Assign Pipe to Prosumer
        'check if prosumer power supply can be satisfied by the remaining prosumers
        IF  $\sum$ P_con(DistributionPipeLeft; DistributionPipeRight) < Ppro_Pro_pipe
            THEN
                Q_max_pro =  $\sum$ P_con(DistributionPipeLeft; DistributionPipeRight)
            ELSE
                Q_max_pro = Ppro_Pro_pipe
            END IF
        'check if prosumer power demand can be satisfied by the remaining prosumers
        IF  $\sum$ P_pro(DistributionPipeLeft; DistributionPipeRight) < Pcon_Pro_pipe
            THEN
                Q_max_con =  $\sum$ P_pro(DistributionPipeLeft; DistributionPipeRight)
            END IF

        Q_max = MAX(Q_max_con; Q_max_pro)

    END IF

NEXT pipe

```

Volume flow and Pressure drop in pipes

ANE and ONE: Maximum consumption volume flow

```

FOR First_Proc_con to Last_Proc_con

IF Pcon_pros > Q_max(Pros_pipe) Then 'calculate the relevant consumption volume flow for control valves
    V_dot_con_pros = V_dot_pro_max(DistributionPipeLeft) + V_dot_pro_max(DistributionPipeRight)

ELSE
    V_dot_con_pros = V_dot_con_pros(Pcon_pros)

END IF

NEXT Proc_con

```

ANE and ONE: Maximum production volume flow

```

FOR First_Proc_pro to Last_Proc_pro

IF Ppro_pros > Q_max(Pros_pipe) Then 'calculate the relevant production volume flow for pumps
    V_dot_pro_pros = V_dot_con_max(DistributionPipeLeft) + V_dot_con_max(DistributionPipeRight)

ELSE
    V_dot_pro_pros = V_dot_pro_pros(Ppro_pros)

END IF

NEXT Proc_pro

```

ONE: Pressure drop in pipes

```
FOR First_Pros_pro to Last_Pros_pro 'go through all possible production prosumers
  Assign Pros_pro to ConnectionPipe
  IF Ppro_pros = 0 THEN 'check if prosumer is active (was assigned power)
    dP_pros_pro = 0
  ELSE
    FOR First_Pros_con to Last_Pros_con 'go through all possible consumption prosumers
      Assign Pros_con to ConnectionPipe
      IF Pcon_pros = 0 then 'check if prosumer is active (was assigned power)
        dP_pros_pipes = 0
      ELSE
        IF ConnectionPipe(Pros_con) = ConnectionPipe(Pros_pro) OR 'exclude irrelevant pipes for pressure loss
          ConnectionPipe(Pros_con) IsLeftOf ConnectionPipeLeft(Pros_pro) OR
          ConnectionPipe(Pros_con) IsRightOf ConnectionPipeRight(Pros_pro) THEN
            dP_pros_pipes = 0
          ELSE
            FOR First_Pipe to Last_Pipe 'go through all pipes
              IF Pipe = ConnectionPipe(Pros_pro) then 'connection pipe dp of the considered Prosumer
                dP_left = dP_left + dP_pipe
                dP_right = dP_right + dP_pipe
              ELSE
                IF ConnectionPipe(Pros_con) IsLeftOf ConnectionPipe(Pros_pro) AND Pipe = DistributionPipeLeft(Pros_pro)
                OR Pipe = ConnectionPipe(Pros_con) AND ConnectionPipe(Pros_con) IsLeftOf ConnectionPipe(Pros_pro) THEN
                  dP_left = dP_left + dP_pipe 'add relevant pipes for the hydraulic circuits to the left
                ELSE
                  IF ConnectionPipe(Pros_con) IsRightOf ConnectionPipe(Pros_pro) AND Pipe = DistributionPipeRight(Pros_pro)
                  OR Pipe = ConnectionPipe(Pros_con) AND ConnectionPipe(Pros_con) IsRightOf ConnectionPipe(Pros_pro) THEN
                    dP_right = dP_right + dP_pipe 'add relevant pipes for the hydraulic circuits to the right
                  END IF
                END IF
              END IF
            NEXT Pipe
          END IF
        END IF
      END IF
    NEXT Pipe
  END IF
  IF dP_left > dP_right THEN 'choose relevant pressure loss (left side or right side)
    dP_pros_pipes = dP_left
```



```

ELSE
    dP_pros_pipes = dP_right
Write dP_pros_pipes in Matrix 'store pressure loss of the considered connection in a table
    End If
NEXT Pros_con
MAX(dP_pros_pipes(First_Pros_con to Last_Pros_con) = dP_pros 'max pressure loss of all connections for the pump dp
NEXT Pros_pro

```

ANE Pressure drop in Pipes

```

For First_Pros_pro to Last_Pros_pro 'go through all possible production prosumers
    Assign Pros_pro to ConnectionPipe
    FOR First_Pros_con to Last_Pros_con
        Assign Pros_con to ConnectionPipe
        IF ConnectionPipe(Pros_pro) is ConnectionPipe(Pros_con) or Ppro_pros or Pcon_pros = 0 THEN
            dP_pros = 0 'check if prosumer is active (was assigned power) and exclude irrelevant pipes for pressure loss
        ELSE
            FOR First_Pipe to Last_Pipe 'go through all pipes
                IF Pipe = ConnectionPipe(Pros_con) THEN 'connection pipe dp of the considered Prosumer
                    dP_left = dP_left + dP_pipe
                    dP_right = dP_right + dP_pipe
                ELSE
                    IF ConnectionPipe(Pros_con) IsRightOf ConnectionPipe(Pros_pro) AND Pipe IsRightOf ConnectionPipe(Pros_pro)
                        AND Pipe IS DistributionPipe AND Pipe IsLeftOf ConnectionPipe(Pros_con) OR Pipe = ConnectionPipe(Pros_con)
                        AND ConnectionPipe(Pros_con) IsLeftOf ConnectionPipe(Pros_pro) THEN
                            dP_left = dP_left + dP_pipe 'add relevant pipes for the hydraulic circuits to the left
                        ELSE
                            IF ConnectionPipe(Pros_con) IsLeftOf ConnectionPipe(Pros_pro) AND Pipe IsLeftOf ConnectionPipe(Pros_pro)
                                AND Pipe IS DistributionPipe AND Pipe IsRightOf ConnectionPipe(Pros_con) OR Pipe = ConnectionPipe(Pros_con)
                                AND ConnectionPipe(Pros_con) IsRightOf ConnectionPipe(Pros_pro) THEN
                                    dP_right = dP_right + dP_pipe 'add relevant pipes for the hydraulic circuits to the right
                                END IF
                            END IF
                        END IF
                    NEXT Pipe
                END IF
            END IF
        END IF
    NEXT Pros_con
END IF

```

If $dP_{left} > dP_{right}$ Then

$dP_{pros_pipes} = dP_{left}$

Else

$dP_{pros_pipes} = dP_{right}$

Write dP_{pros_pipes} in Matrix 'store pressure loss of the considered connection in a table

End If

Next Pros_con

$MAX(dP_{pros_pipes}(First_Pros_con \text{ to } Last_Pros_con)) = dP_{pros}$ 'max pressure loss of all connections for the pump dp

Next Pros_pro

Component dimensioning

For First_Pros_pro to Last_Pros_pro 'go through all production prosumers

Write dP_{pros} in matrix 'store relevant pressure loss for the pump dp in a table

Calculate $dp_{fittings}$ 'apply chosen method for fitting dp

For First_Pros_con to Last_Pros_con

'CoV dimensioning for all consumption prosumers

LOOKUP valveauthority and $dp_{substation}$

Calculate dp_{valve_theo}

Calculate Kv_{valve}

Choose Kvs_value

Calculate dp_{valve_real}

Write CoV design values in Matrix

Next Pros_con

'FIP dimensioning for all production prosumers

LOOKUP dp_{valve_real}

LOOKUP max dp_{Pros}

Calculate H_{FIP_max}

LOOKUP $V_{dot_con_max_pros}$

Write FIP design values in Matrix

Next Pros_pro

C. Simulation parameters

Table C.1: Set power transfers (exchange scenarios) at the prosumer substations in the simulation
negative value: consumption-mode, positive value: Production-mode

	Prosumer 1	Prosumer 2	Prosumer 3	Prosumer 4	Prosumer 5
Time in	Qdot_set in	Qdot_set in	Qdot_set in	Qdot_set in	Qdot_set in
s	kW	kW	kW	kW	kW
0	12.64	10.75	8.15	-20.91	-10.62
900	12.64	10.75	8.15	-20.91	-10.62
1800	12.64	10.75	8.15	-20.91	-10.62
2700	12.64	10.75	8.15	-20.91	-10.62
3600	25.27	21.51	16.29	-41.83	-21.24
4500	25.27	21.51	16.29	-41.83	-21.24
5400	25.27	21.51	16.29	-41.83	-21.24
6300	25.27	21.51	16.29	-41.83	-21.24
7200	12.64	10.75	8.15	-20.91	-10.62
8100	-12.64	-10.75	-8.15	20.91	10.62
9000	-25.27	-21.51	-16.29	41.83	21.24
9900	-25.27	-21.51	-16.29	41.83	21.24
10800	-25.27	-21.51	-16.29	41.83	21.24
11700	-25.27	-21.51	-16.29	41.83	21.24
12600	-12.64	-10.75	-8.15	20.91	10.62
13500	-12.64	-10.75	10.62	6.38	6.38
14400	-25.27	-21.51	21.24	12.77	12.77
15300	-25.27	-21.51	21.24	12.77	12.77
16200	-25.27	-21.51	21.24	12.77	12.77
17100	-25.27	-21.51	21.24	12.77	12.77
18000	-12.64	-10.75	10.62	6.38	6.38
18900	12.64	10.75	-10.62	-6.38	-6.38
19800	25.27	21.51	-21.24	-12.77	-12.77
20700	25.27	21.51	-21.24	-12.77	-12.77
21600	25.27	21.51	-21.24	-12.77	-12.77
22500	25.27	21.51	-21.24	-12.77	-12.77
23400	12.64	10.75	-10.62	-6.38	-6.38
24300	6.32	5.38	4.07	-10.46	-5.31
25200	12.64	10.75	8.15	-20.91	-10.62
26100	12.64	10.75	8.15	-20.91	-10.62
27000	12.64	10.75	8.15	-20.91	-10.62
27900	12.64	10.75	8.15	-20.91	-10.62
28800	6.32	5.38	4.07	-10.46	-5.31
29700	-6.32	-5.38	-4.07	10.46	5.31
30600	-12.64	-10.75	-8.15	20.91	10.62
31500	-12.64	-10.75	-8.15	20.91	10.62
32400	-12.64	-10.75	-8.15	20.91	10.62
33300	-12.64	-10.75	-8.15	20.91	10.62

Table C.2: Applied parameters for the ProsNet [51] models and PID controllers [54] in the Dymola simulation

Parameter	Prosumer 1	Prosumer 2	Prosumer 3	Prosumer 4	Prosumer 5	Unit
CTRL PID Q_T_weighted						
Delta_Qdot_norm	1	1	1	1	1	
Delta_T_norm	3	3	3	3	3	K
T_prim_hot_des	65	65	65	65	65	°C
T_sec_hot_des	60	60	60	60	60	°C
DeltaT_prim_des	15	15	15	15	15	K
DeltaT_sec_des	15	15	15	15	15	K
V_dot_sec_max	29.02	24.70	24.40	48.03	24.40	l/min
k_prim_prod	1.5	1.5	1.5	1.5	1.5	
Ti_prim_prod	35	35	35	35	35	s
Td_prim_prod	0.1	0.1	0.1	0.1	0.1	s
heat transfer station						
Q_flow_nominal	30327	25809	25494	50192	25494	W
T_a1_nominal	65	65	65	65	65	°C
T_a2_nominal	45	45	45	45	45	°C
m_flow_nominal_1	0.40	0.34	0.34	0.67	0.34	kg/s
dp1_nominal	0.2	0.2	0.2	0.2	0.2	bar
m_flow_nominal_2	0.40	0.34	0.34	0.67	0.34	kg/s
dp2_nominal	0.2	0.2	0.2	0.2	0.2	bar
Kv_conVal	1.6	1.6	1.6	2.5	1.6	m ³ h/bar ^(1/2)
l_conVal	2.00E-03	2.00E-03	2.00E-03	0.002	2.00E-03	
Kv_cheVal	11	11	11	20	11	m ³ h/bar ^(1/2)
l_cheVal	0.001	0.001	0.001	0.001	0.001	
Transfer station pipes						
length_transfer_pipe_tot	20	20	20	20	20	m
zeta_transferstation	15.02	15.07	15.07	19.40	15.07	
d_transferpipe	0.0273	0.0273	0.0273	0.036	0.0273	m
R_ins_transferpipe	1000	1000	1000	1000	1000	Km/W
Valve_prim_con_Parameters						
R	50	50	50	50	50	-
delta0	0.01	0.01	0.01	0.01	0.01	-
Dynamics						
Feed-in pump						
tau_feedPump	3	3	3	3	3	s
use_inputFilter_feedPump	true	true	true	true	true	
riseTime_feedPump	35	35	35	35	35	s
y_start_feedPump	0	0	0	0	0	
Control valve						
use_inputFilter_conVal	true	true	true	true	true	
riseTime_conVal	35	35	35	35	35	s
y_start_conVal	1	1	1	1	1	
Secondary side pumps dynamics						
tau_pumpsSec	3	3	3	3	3	s
use_inputFilter_pumpsSec	true	true	true	true	true	
riseTime_pumpsSec	35	35	35	35	35	s
m_flow_start_pumpsSec	0	0	0	0	0	kg/s
y_start_pumpsSec	1	1	1	1	1	
Secondary side control volume dynamics						
tau_cv	10	10	10	10	10	s
T_start_cv	60	60	60	60	60	°C
Network pipes						
	Pipe_12	Pipe_23	Pipe_34	Pipe_45	-	
R_ins_transferpipe	1000	1000	1000	1000		Km/W
length	40	40	49.5	46.5		m
diameter	0.0273	0.036	0.0419	0.0273		mm
zeta	7.18	5.03	5.17	8.60		-